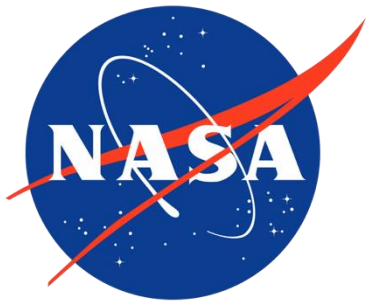
A Predictive Wall Model for Laminar-Turbulent Transition for Large-Eddy Simulation in External Aerodynamics

Carlos A. Gonzalez

Advanced Modeling & Simulation (AMS) Seminar Series
NASA Ames Research
June 4th, 2026

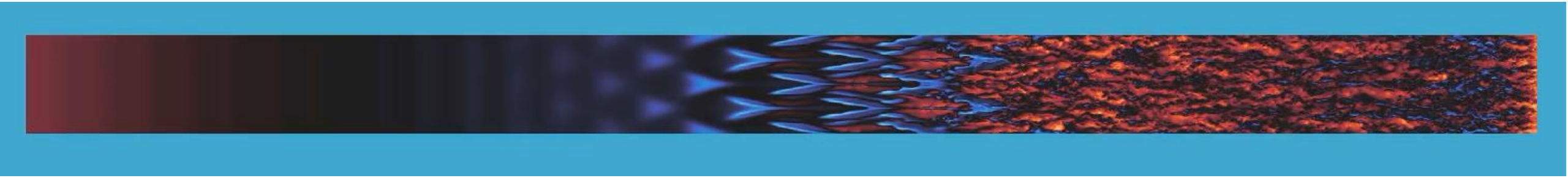




OAK RIDGE National Laboratory | LEADERSHIP COMPUTING FACILITY

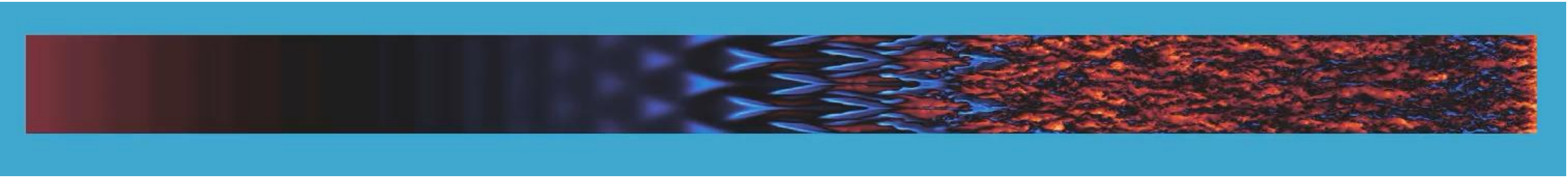
Transitional Flows

- Transitional flows are those which exhibit laminar, transitional, and turbulent behavior



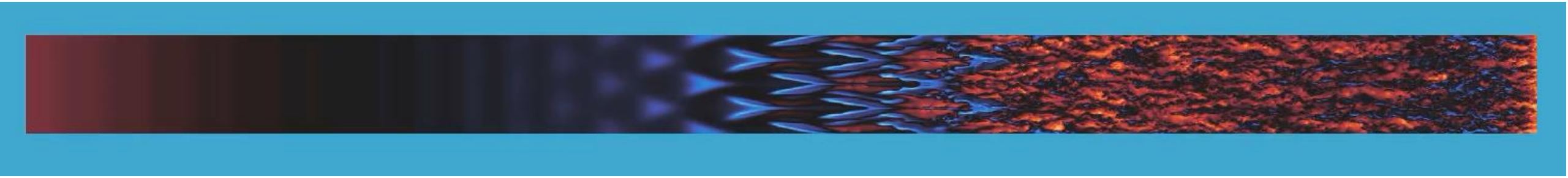
Transitional Flows

- Transitional flows are those which exhibit laminar, transitional, and turbulent behavior
- Transition to turbulence is associated with dramatically increased skin-friction and surface heat transfer



Transitional Flows

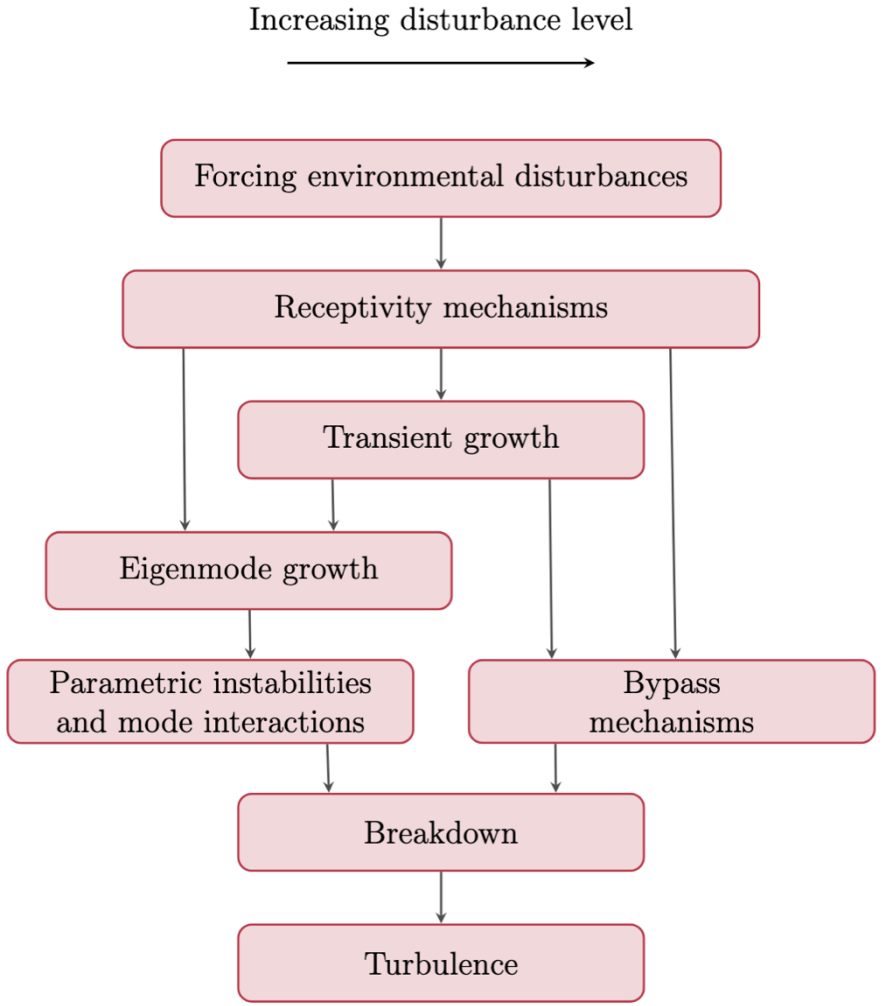
- Transitional flows are those which exhibit laminar, transitional, and turbulent behavior
- Transition to turbulence is associated with dramatically increased skin-friction and surface heat transfer
- Renewed interest from industry and academia in the application of natural-laminar-flow airfoils that delay the onset of transition as compared to traditionally used airfoil shapes



Transition Modeling Approaches

- The focus on this work is on natural transition
  - Common in external aerodynamics

- Many approaches exist for modeling transition: e^N methods[1], RANS type models[2], Data-driven methods[3]



[1] J. Van Ingen. A suggested semi-empirical method for the calculation of the boundary layer transition region. University of Techn., Dept. of Aerospace Eng., Report UTH-74, 1956
[2] Langtry, R., & Menter, F. (2005, January). In 43rd AIAA aerospace sciences meeting and exhibit (p. 522).
[3] Duraisamy, K., & Durbin, P. (2014). Transition modeling using data driven approaches. In *Proceedings of the CTR Summer Program* (p. 427).

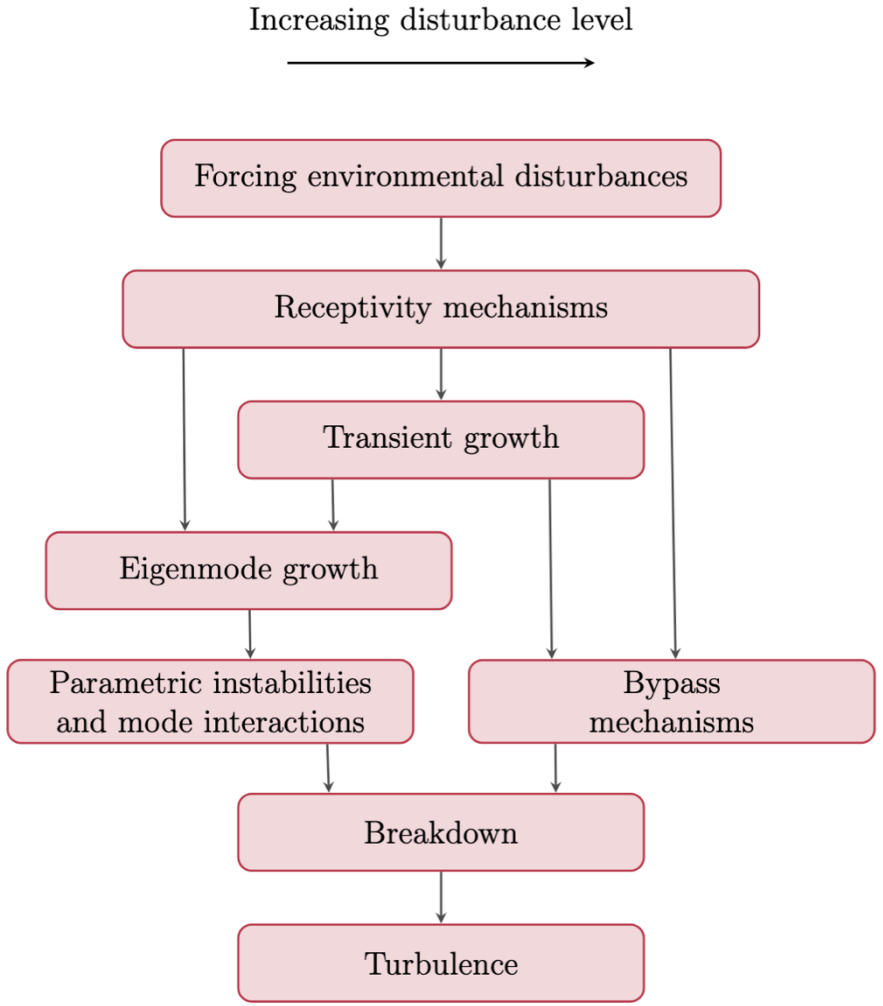
Transition Modeling Approaches

- The focus on this work is on natural transition
  - Common in external aerodynamics

- Many approaches exist for modeling transition: e^N methods[1], RANS type models[2], Data-driven methods[3]

- **These methods are *ad-hoc* and require tuning!**

- Our goal is to develop a more physics-based approach

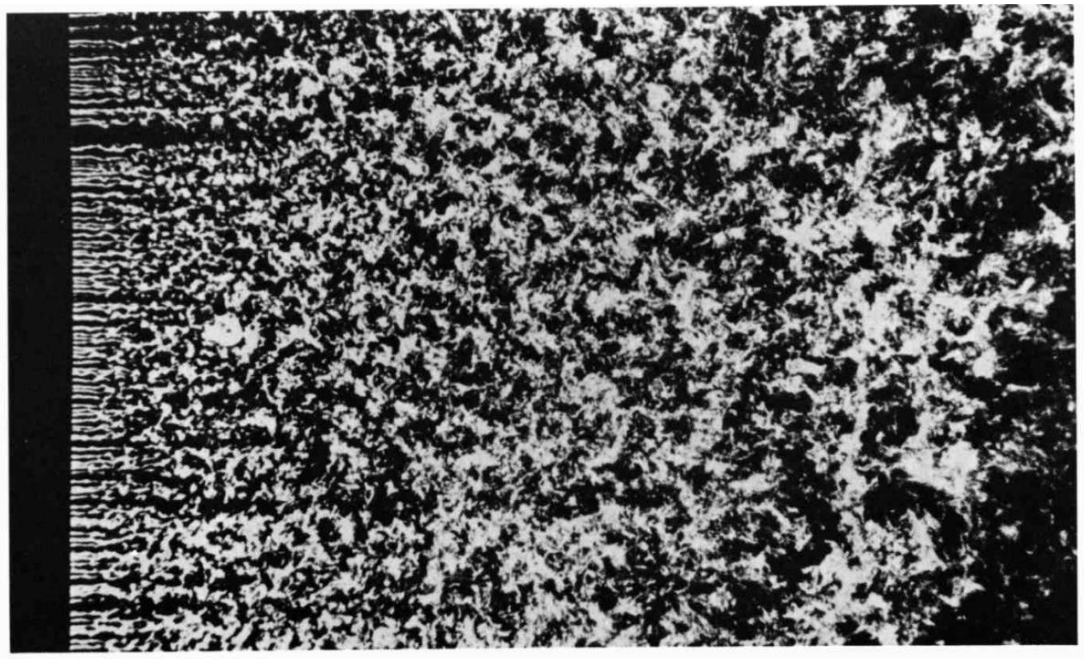


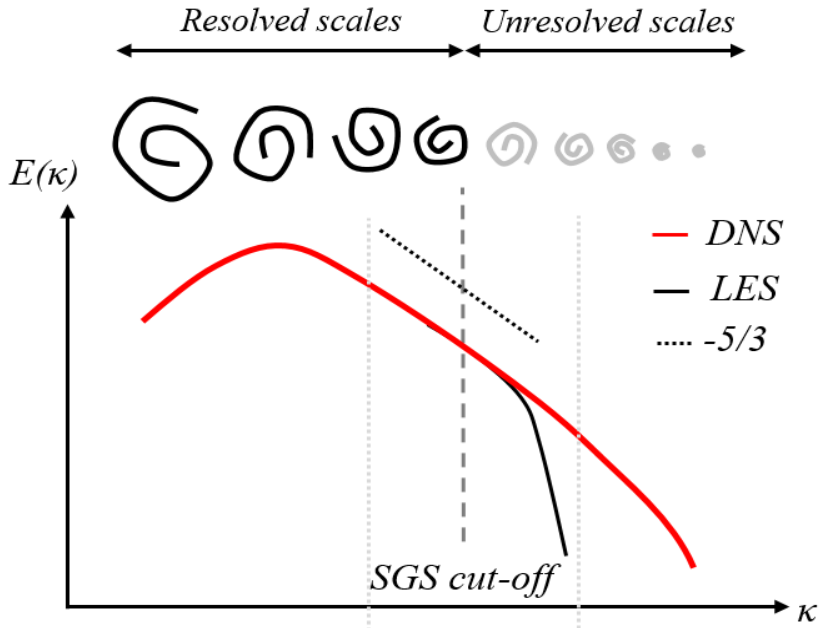
[1] J. Van Ingen. A suggested semi-empirical method for the calculation of the boundary layer transition region. University of Techn., Dept. of Aerospace Eng., Report UTH-74, 1956
[2] Langtry, R., & Menter, F. (2005, January). In 43rd AIAA aerospace sciences meeting and exhibit (p. 522).
[3] Duraisamy, K., & Durbin, P. (2014). Transition modeling using data driven approaches. In *Proceedings of the CTR Summer Program* (p. 427).

Turbulence Modeling and Simulation

- Turbulent flow introduces a range of energetic scales

- Direct numerical simulation, i.e. resolving the full range of scales is unaffordable for problems of practical engineering interest
  - › Large-eddy simulation proposes to resolve the largest and most energetic turbulent flow structures and model the small “subgrid” ones

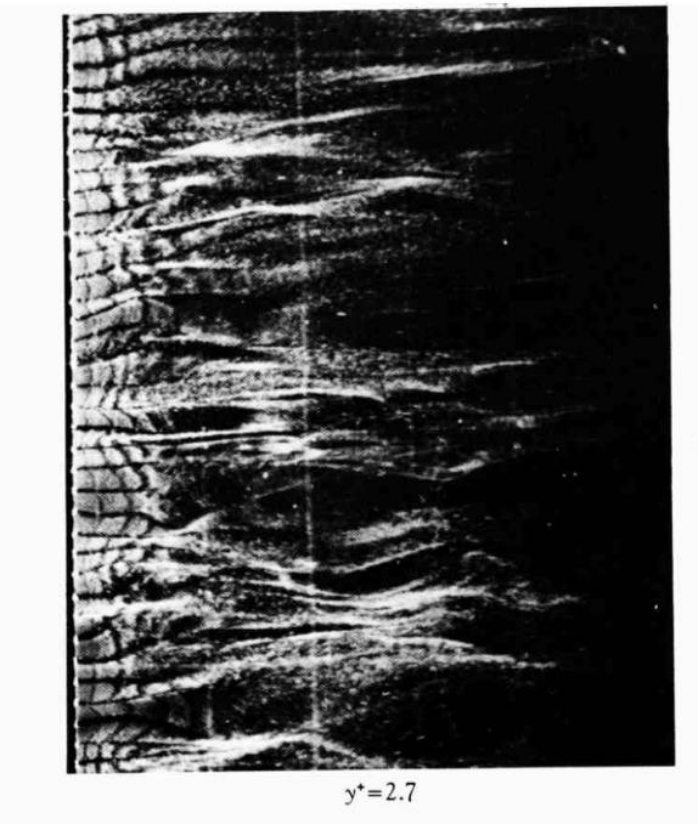




Van Dyke, M. (1982). An album of fluid motion. *NASA STI/Recon Technical Report A*, *82*, 36549.

Near-wall Turbulence

- For wall-bounded flows, the energetic turbulent structures become increasingly small as the flow approaches the wall

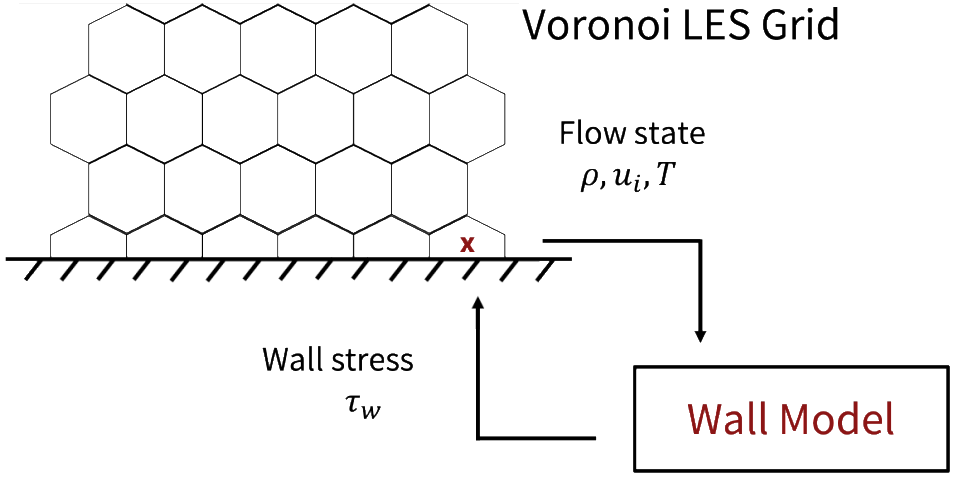


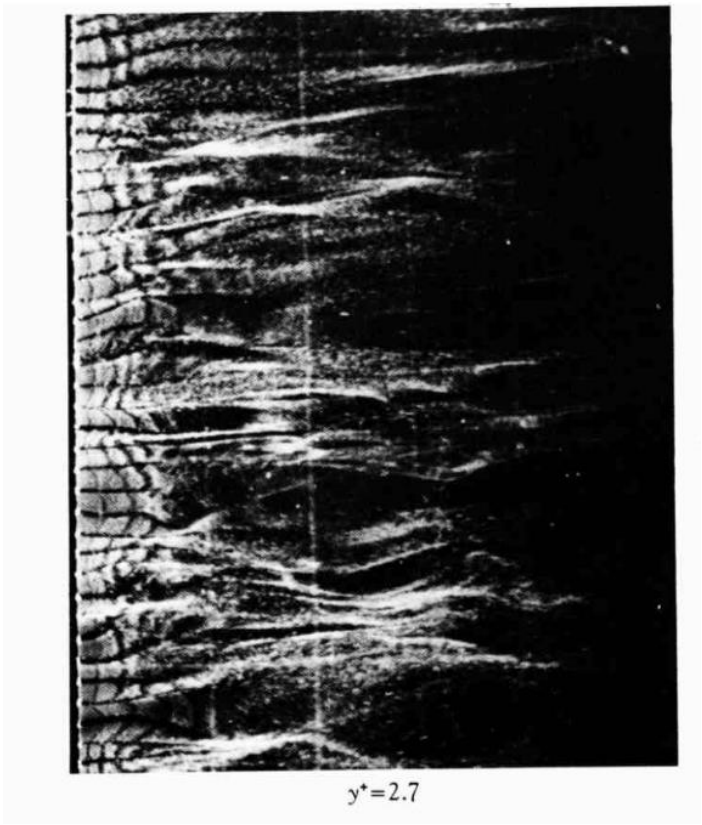
Bose, S. T., & Park, G. I. (2018). Wall-modeled large-eddy simulation for complex turbulent flows. Annual review of fluid mechanics, 50, 535-561.
Van Dyke, M. (1982). An album of fluid motion. *NASA STI/Recon Technical Report A*, *82*, 36549.

Near-wall Turbulence

- For wall-bounded flows, the energetic turbulent structures become increasingly small as the flow approaches the wall

- Wall-modeled LES has been developed as a simulation and modeling technique to overcome the resolution requirements imposed by the near-wall structures
  - Equilibrium turbulent boundary layer assumptions are invoked to model the near-wall eddies



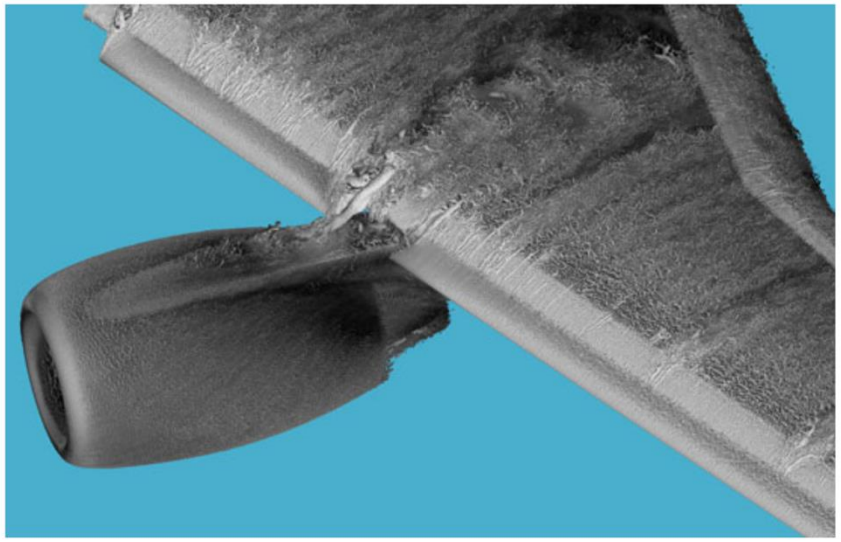


Bose, S. T., & Park, G. I. (2018). Wall-modeled large-eddy simulation for complex turbulent flows. Annual review of fluid mechanics, 50, 535-561.
Van Dyke, M. (1982). An album of fluid motion. *NASA STI/Recon Technical Report A*, *82*, 36549.

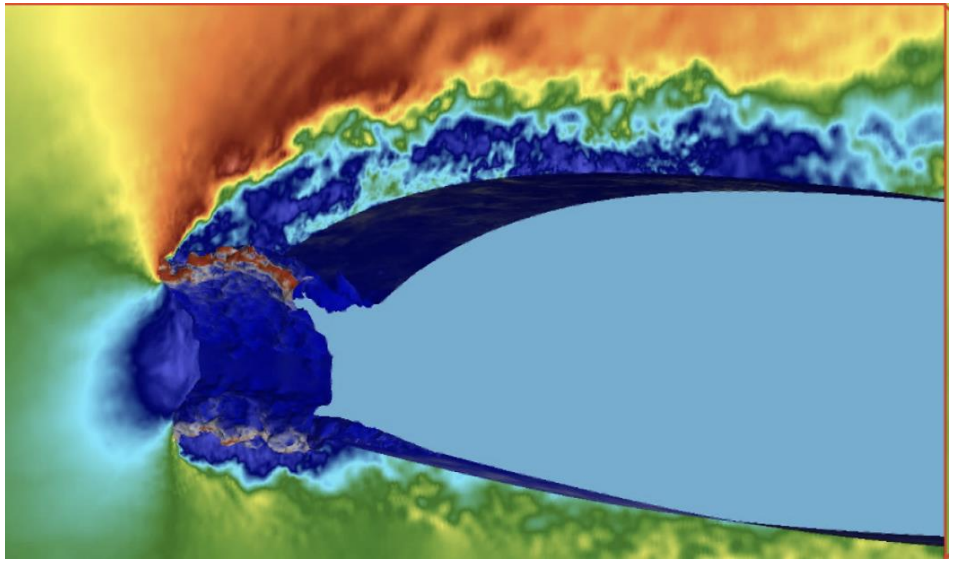
Introduction to WMLES

- WMLES has recently been successful at simulating turbulent flows of engineering interest
  - Complex geometries
  - Unsteady flows
  - Separation

JAXA Standard Model



Horn ice airfoil WMLES

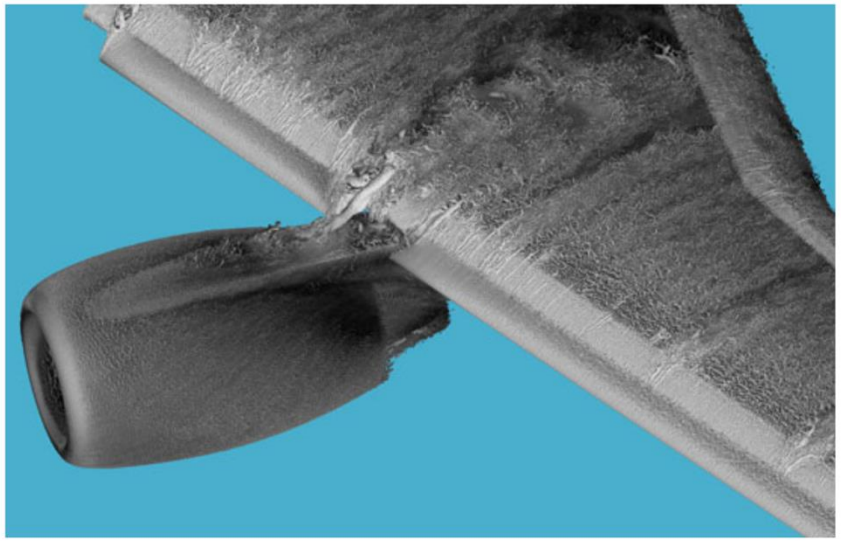


[1] Agrawal, R., Whitmore, M. P., Griffin, K. P., Bose, S. T., & Moin, P. (2022). Non-Boussinesq subgrid-scale model with dynamic tensorial coefficients. Physical Review Fluids, 7(7), 074602.
[2] B. Bornhoft, P. Moin, S. S. Jain, and S. T. Bose. On the use of artificial ice shapes for large-eddy simulations in aircraft icing. Journal of Aircraft, pages 1–18, 2025.
[3] Goc, K. A., Lehmkuhl, O., Park, G. I., Bose, S. T., & Moin, P. (2021). Large eddy simulation of aircraft at affordable cost: a milestone in computational fluid dynamics. Flow, 1, E14.

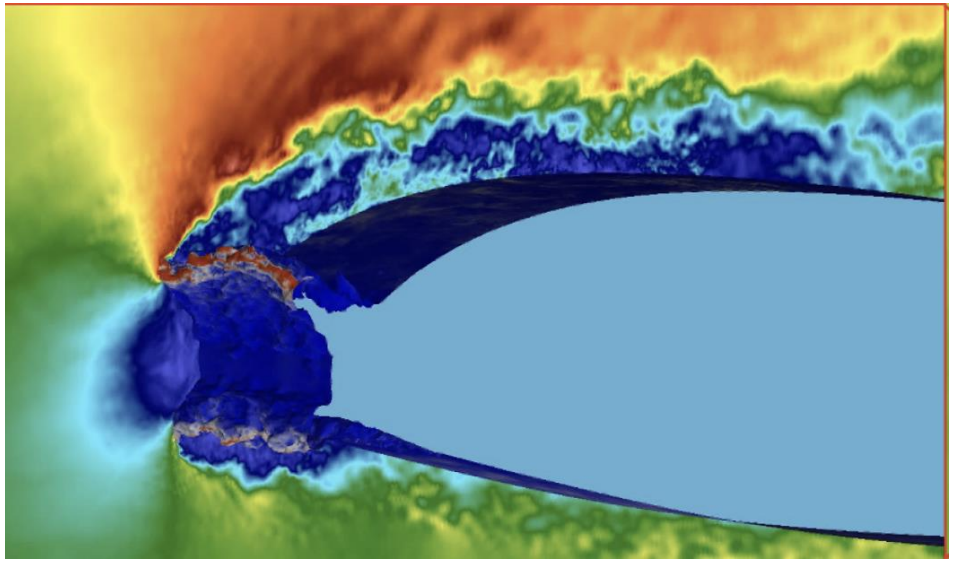
Introduction to WMLES

- WMLES has recently been successful at simulating turbulent flows of engineering interest
  - Complex geometries
  - Unsteady flows
  - Separation

JAXA Standard Model



Horn ice airfoil WMLES



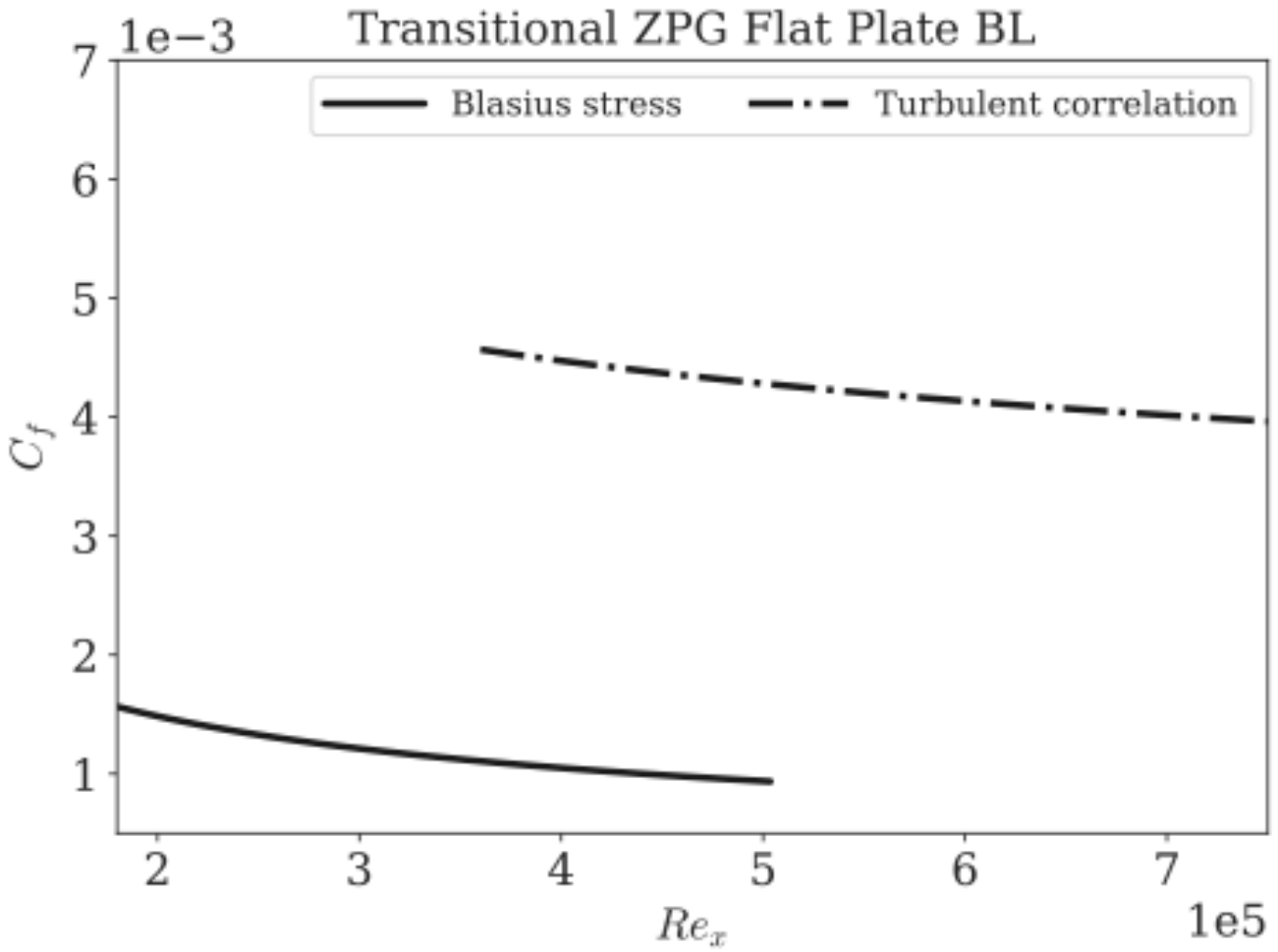
But WMLES has not worked for transitional flows!

[1] Agrawal, R., Whitmore, M. P., Griffin, K. P., Bose, S. T., & Moin, P. (2022). Non-Boussinesq subgrid-scale model with dynamic tensorial coefficients. Physical Review Fluids, 7(7), 074602.

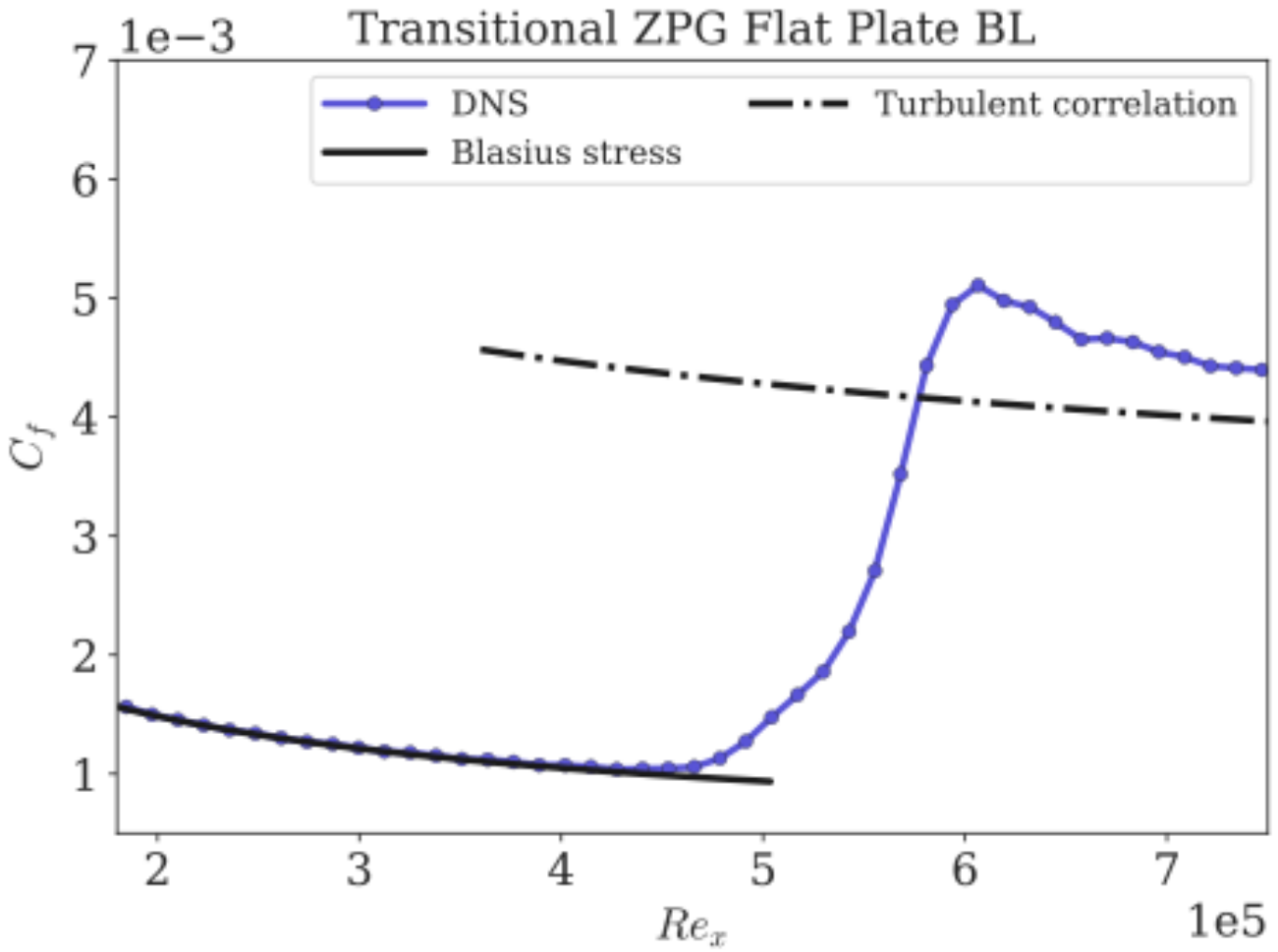
[2] B. Bornhoft, P. Moin, S. S. Jain, and S. T. Bose. On the use of artificial ice shapes for large-eddy simulations in aircraft icing. Journal of Aircraft, pages 1–18, 2025.

[3] Goc, K. A., Lehmkuhl, O., Park, G. I., Bose, S. T., & Moin, P. (2021). Large eddy simulation of aircraft at affordable cost: a milestone in computational fluid dynamics. Flow, 1, E14.

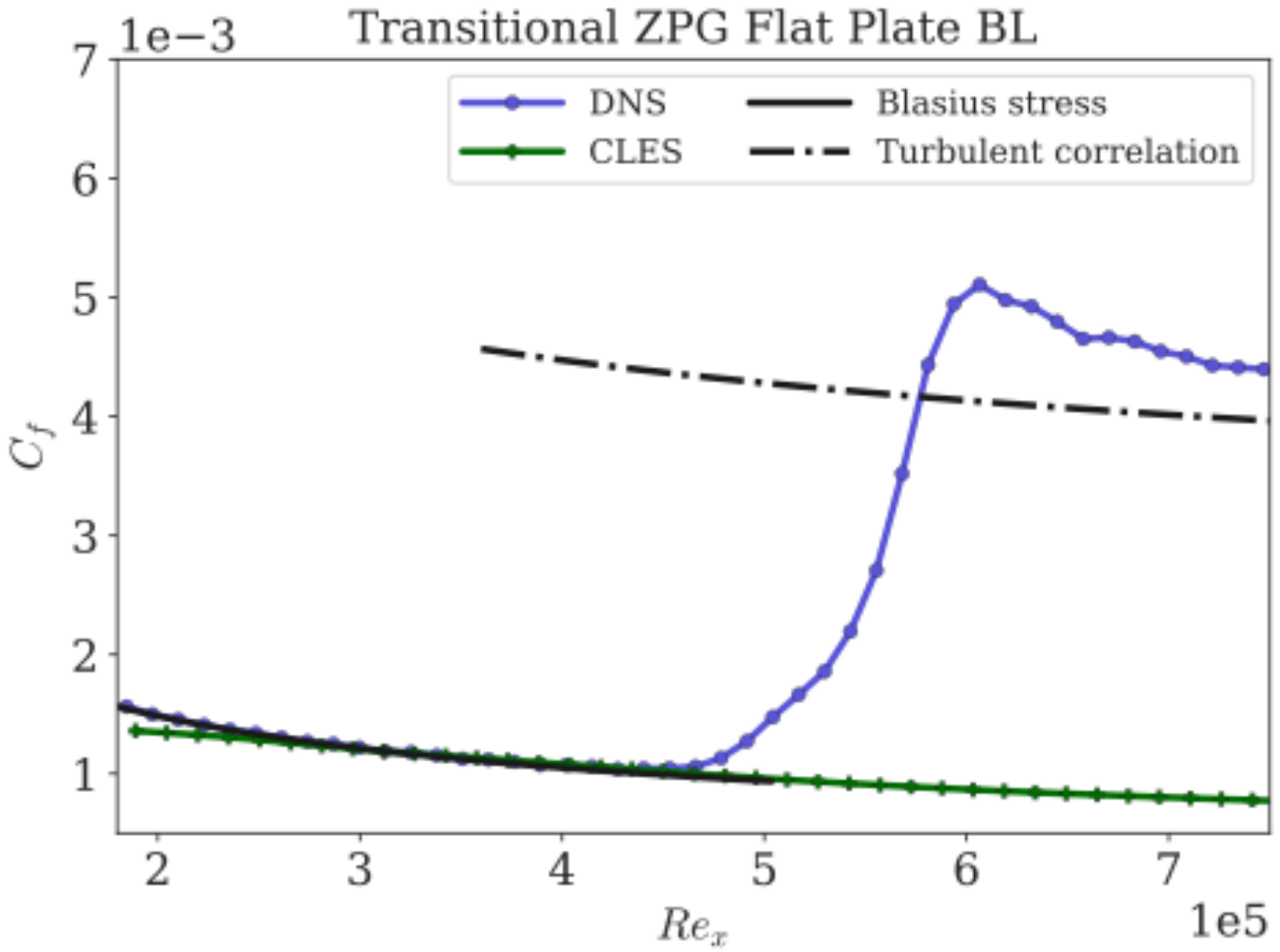
WMLES of Transitioning Flows



WMLES of Transitioning Flows

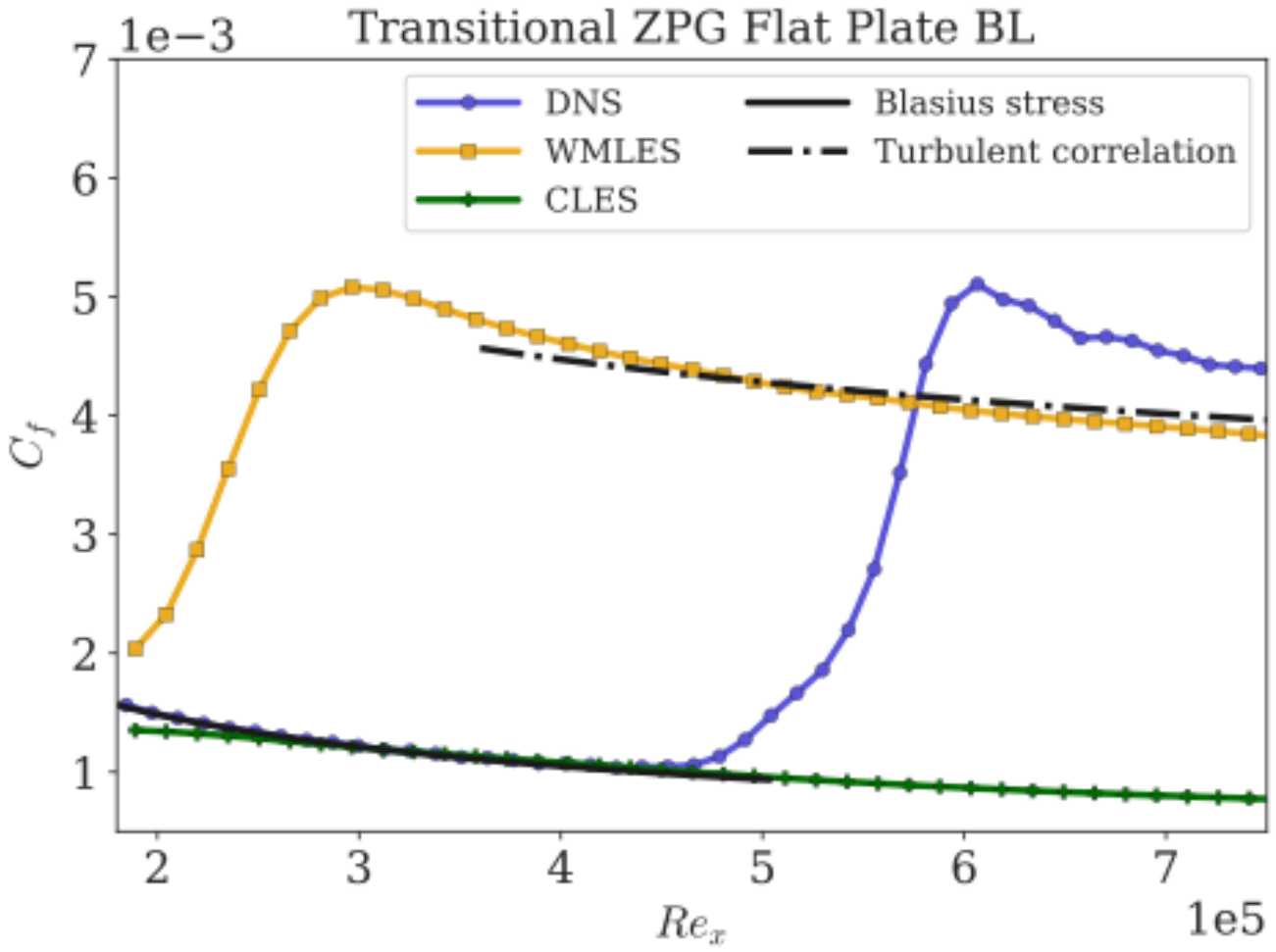


WMLES of Transitioning Flows



WMLES of Transitioning Flows

- WMLES does not reliably predict laminar and transitional flows!



Cost of WMLES for Transition

- WMLES can require **10 to 100 times** more grid points in the thin laminar region than in the turbulent regime to properly capture the instabilities preceding transition[1]

2D NACA0012 Estimation[1]		
Re_c	N^{lam}	N^{turb}
$1E6$	$1.1E6$	$1.3E4$
$1E7$	$1.1E7$	$1.5E5$
$1E8$	$9.1E7$	$3.1E6$

[1] Slotnick, J. P., Khodadoust, A., Alonso, J., Darmofal, D., Gropp, W., Lurie, E., & Mavriplis, D. J. (2014). CFD vision 2030 study: a path to revolutionary computational aerosciences (No. NF1676L-18332).

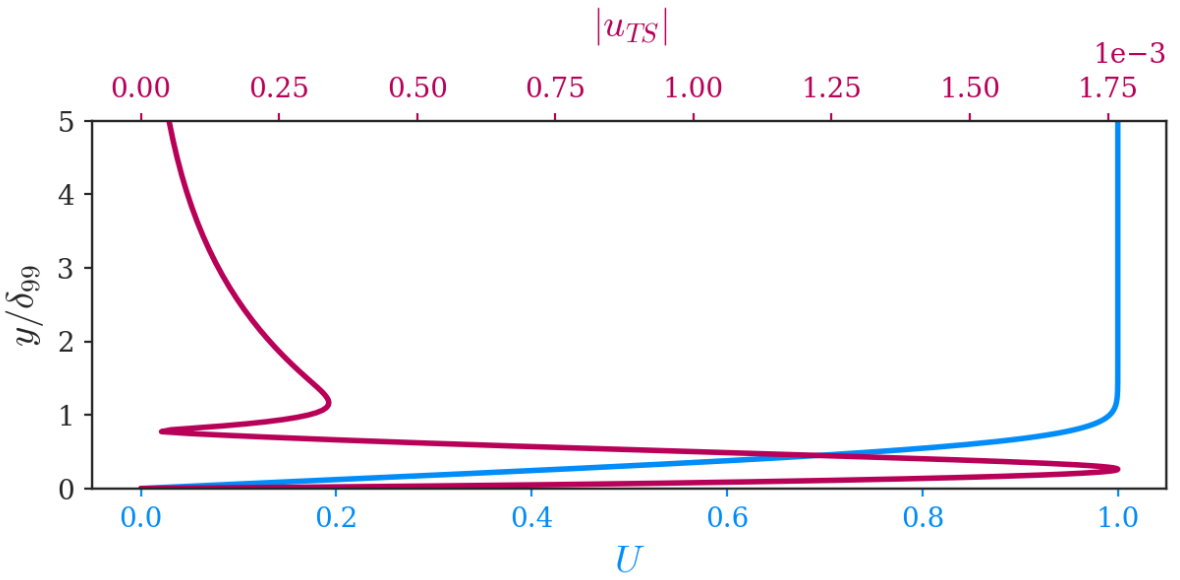
Cost of WMLES for Transition

- WMLES can require **10 to 100 times** more grid points in the thin laminar region than in the turbulent regime to properly capture the instabilities preceding transition[1]

- Natural transition requires resolving the laminar base flow and the primary disturbance in the flow
  - Tollmien-Schlicting (TS) wave

- Realistic aircraft simulations can have boundary layer thickness $\delta_{99} \approx O(0.1mm)$ and $L \approx O(10m)$

2D NACA0012 Estimation[1]		
Re_c	N^{lam}	N^{turb}
$1E6$	$1.1E6$	$1.3E4$
$1E7$	$1.1E7$	$1.5E5$
$1E8$	$9.1E7$	$3.1E6$



[1] Slotnick, J. P., Khodadoust, A., Alonso, J., Darmofal, D., Gropp, W., Lurie, E., & Mavriplis, D. J. (2014). CFD vision 2030 study: a path to revolutionary computational aerosciences (No. NF1676L-18332).

Overview



Laminar | Transitional | Turbulent

(1) Development of Falkner-Skan Wall Model

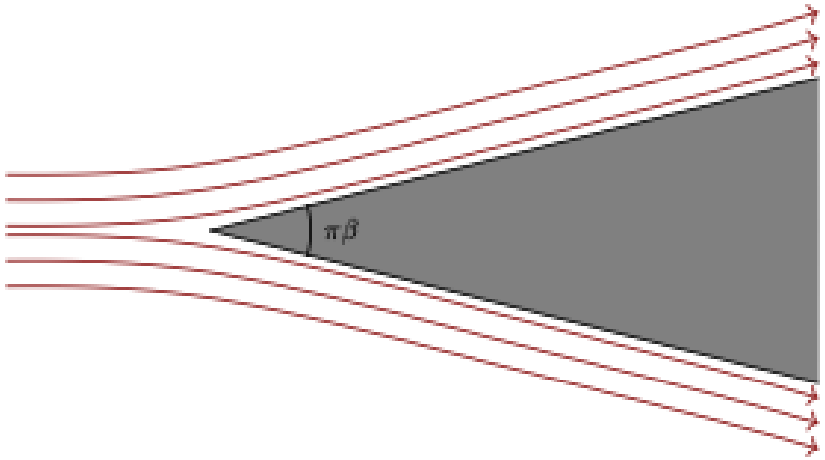
(2) Transition modeling with nonlinear parabolized stability equations

(3) Constructing WMLES inflow conditions from NLPSE

(4) Fully integrated PSE-Sponge simulations of transitional flows

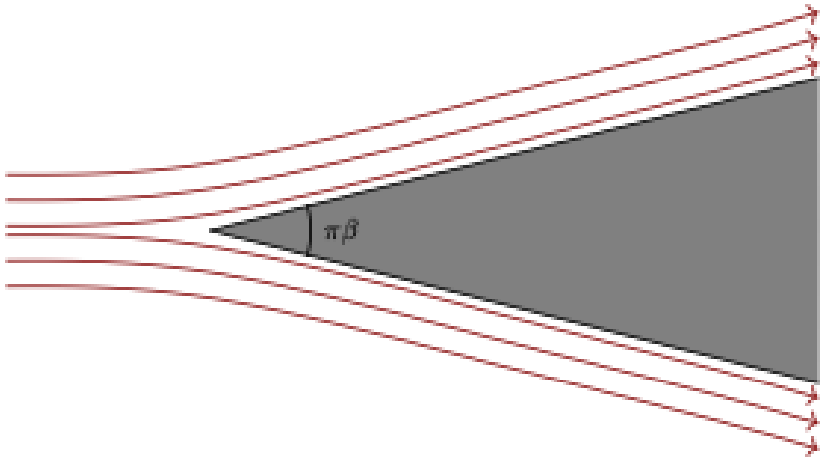
The Falkner-Skan Wall Model for Laminar Flows

- The Falkner-Skan boundary layer described the steady 2D laminar boundary layer that forms on a wedge
  - It is a generalization of the Blasius boundary layer



The Falkner-Skan Wall Model for Laminar Flows

- The Falkner-Skan boundary layer described the steady 2D laminar boundary layer that forms on a wedge
  - It is a generalization of the Blasius boundary layer



- By assuming a power law velocity $U_e = kx^m$ one can find a similarity solution to the boundary layer equations as

$$f''' + ff'' + \beta[1 - (f')^2] = 0$$

$$\beta = \frac{2m}{1+m} \qquad \eta = y\sqrt{\frac{m+1}{2}\frac{U_e}{\nu x}}$$

The Falkner-Skan Wall Model for Laminar Flows

- We propose that laminar boundary layers are locally self-similar
  - This enables us to use geometrical and free-stream information to reconstruct local BL profiles and apply a Falkner-Skan stress at the wall

	EQWM	FSWM
Governing ODE	$\frac{d}{dy}\left[\left(\mu+\mu_{t,wm}\right)\frac{dU}{dy}\right]=0$	$f'''+ff''+\beta[1-(f')^2]=0$
Shear Stress Equation	$\tau_w=\mu\frac{dU}{dy}$	$\tau_w=\mu\left(\frac{m+1}{2}\right)^{\frac{1}{2}}\left(\frac{U_e^3}{\nu\, x}\right)^{\frac{1}{2}}f''(0)$

Griffin, K. P., Fu, L., & Moin, P. (2021). General method for determining the boundary layer thickness in nonequilibrium flows. Physical Review Fluids, 6(2), 024608.

Gonzalez, C. A., Karp, M., & Moin, P. (2020). Wall-stress modeling for laminar boundary layers in coarse grids. Annual Research Briefs, Center for Turbulence Research, Stanford University, 85-95.

The Falkner-Skan Wall Model for Laminar Flows

- We propose that laminar boundary layers are locally self-similar
  - This enables us to use geometrical and free-stream information to reconstruct local BL profiles and apply a Falkner-Skan stress at the wall
  - β is the angle between the surface parallel direction and the free-stream flow direction and can be found geometrically

	EQWM	FSWM
Governing ODE	$\frac{d}{dy}\left[\left(\mu+\mu_{t,wm}\right)\frac{dU}{dy}\right]=0$	$f'''+ff''+\beta[1-(f')^2]=0$
Shear Stress Equation	$\tau_w=\mu\frac{dU}{dy}$	$\tau_w=\mu\left(\frac{m+1}{2}\right)^{\frac{1}{2}}\left(\frac{U_e^3}{\nu\, x}\right)^{\frac{1}{2}}f''(0)$

Griffin, K. P., Fu, L., & Moin, P. (2021). General method for determining the boundary layer thickness in nonequilibrium flows. Physical Review Fluids, 6(2), 024608.

Gonzalez, C. A., Karp, M., & Moin, P. (2020). Wall-stress modeling for laminar boundary layers in coarse grids. Annual Research Briefs, Center for Turbulence Research, Stanford University, 85-95.

The Falkner-Skan Wall Model for Laminar Flows

- We propose that laminar boundary layers are locally self-similar
  - This enables us to use geometrical and free-stream information to reconstruct local BL profiles and apply a Falkner-Skan stress at the wall
  - β is the angle between the surface parallel direction and the free-stream flow direction and can be found geometrically
  - Local values of the free-stream velocity $U_e(x)$ can be found using boundary layer probes using the method of Griffin et al.

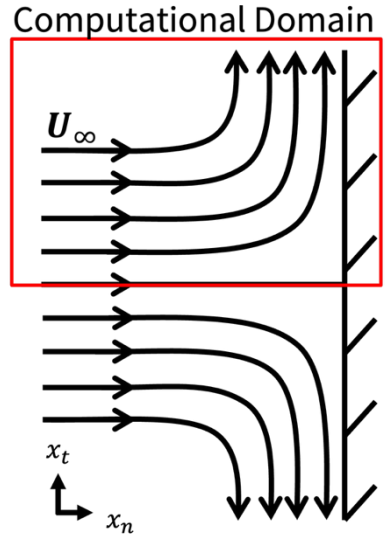
	EQWM	FSWM
Governing ODE	$\frac{d}{dy}\left[(\mu + \mu_{t,wm})\frac{dU}{dy}\right] = 0$	$f''' + ff'' + \beta[1 - (f')^2] = 0$
Shear Stress Equation	$\tau_w = \mu\frac{dU}{dy}$	$\tau_w = \mu\left(\frac{m+1}{2}\right)^{\frac{1}{2}}\left(\frac{U_e^3}{\nu\, x}\right)^{\frac{1}{2}} f''(0)$

Griffin, K. P., Fu, L., & Moin, P. (2021). General method for determining the boundary layer thickness in nonequilibrium flows. Physical Review Fluids, 6(2), 024608.

Gonzalez, C. A., Karp, M., & Moin, P. (2020). Wall-stress modeling for laminar boundary layers in coarse grids. Annual Research Briefs, Center for Turbulence Research, Stanford University, 85-95.

Stagnation Flow

- Uniform flow impinging on a perpendicular flat plate
  - Stagnation flow is an exact solution to the Falkner-Skan equation for the case of $\beta = m = 1$

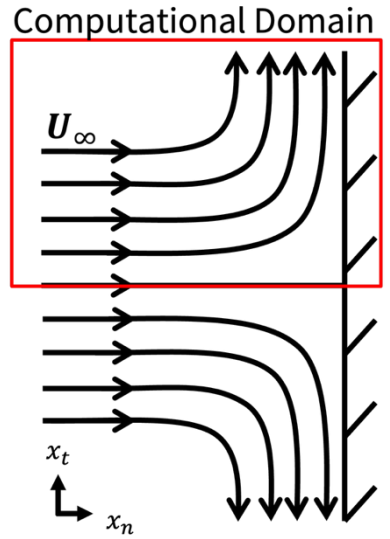


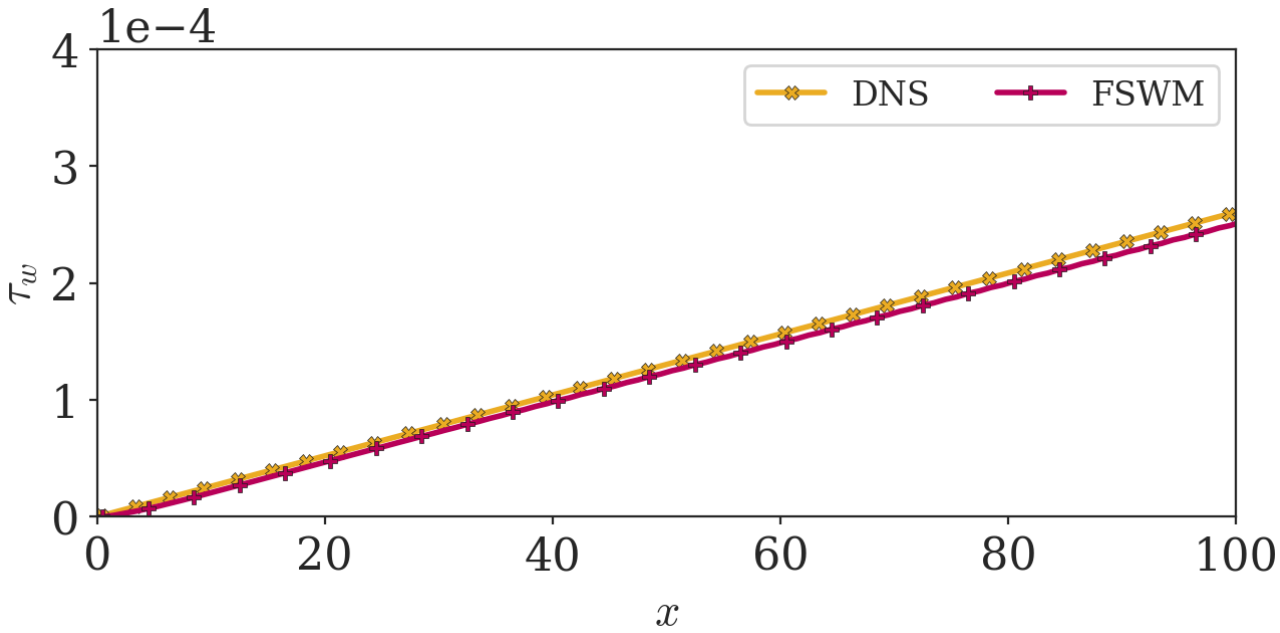
Gonzalez, C. A., Karp, M., & Moin, P. (2020). Wall-stress modeling for laminar boundary layers in coarse grids. Annual Research Briefs, Center for Turbulence Research, Stanford University, 85-95.

Stagnation Flow

- Uniform flow impinging on a perpendicular flat plate
  - Stagnation flow is an exact solution to the Falkner-Skan equation for the case of $\beta = m = 1$

- FSWM boundary condition implemented in charLES
  - $N_n = 5 \times N_s = 150$
    - Entirely subgrid boundary layer

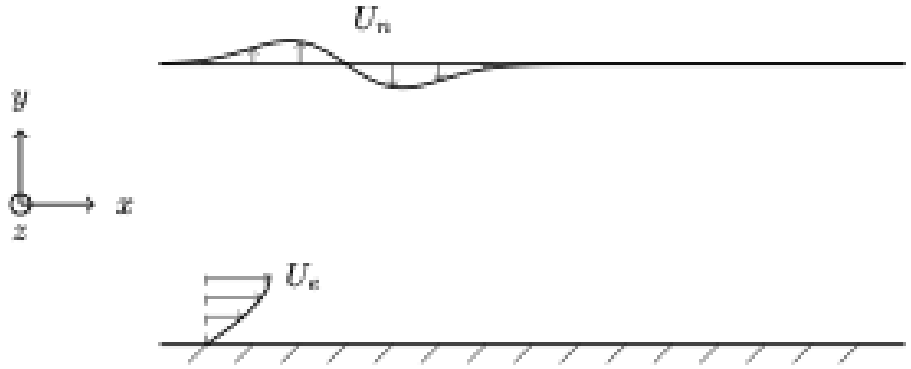




Gonzalez, C. A., Karp, M., & Moin, P. (2020). Wall-stress modeling for laminar boundary layers in coarse grids. Annual Research Briefs, Center for Turbulence Research, Stanford University, 85-95.

Pressure Gradient Boundary Layer

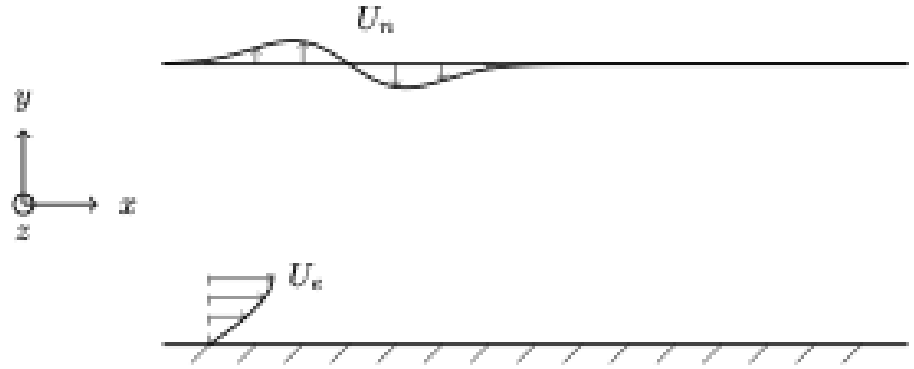
- To test the FSWM in a more general setting, we applied it to flow over a flat plate with a spatially varying edge pressure gradient.
  - Assess the validity of the local self-similarity assumption for a more general flow
  - Exponentially growing and decaying wall-normal velocity distribution is prescribed on the top boundary of the computational domain to create a varying pressure distribution



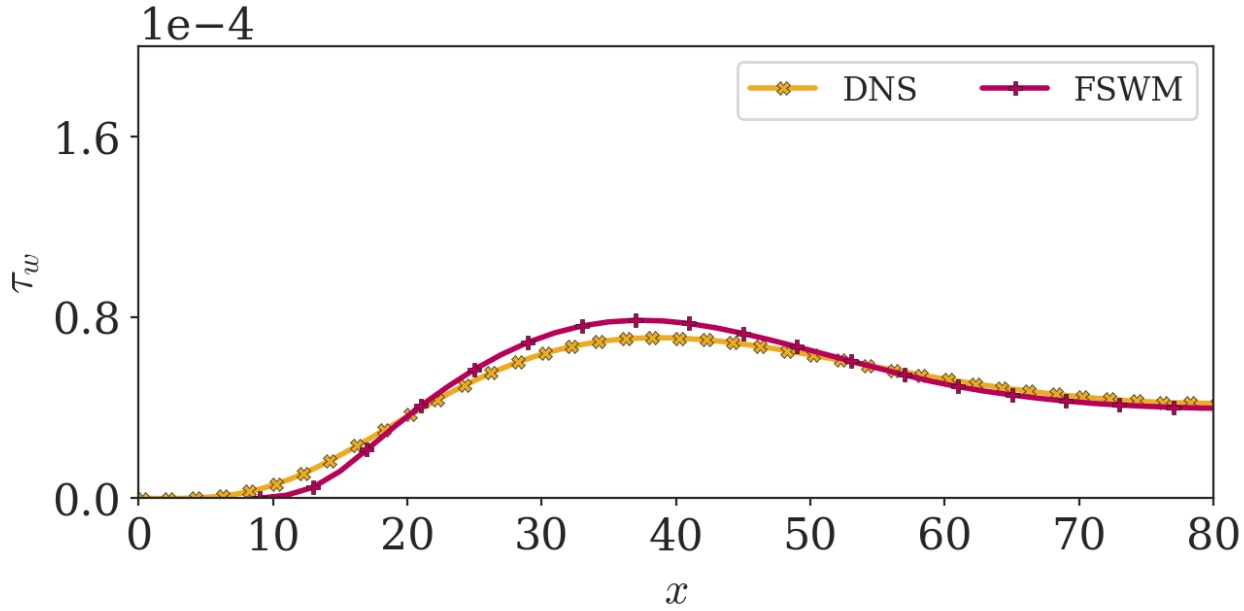
Gonzalez, C. A., Karp, M., & Moin, P. (2020). Wall-stress modeling for laminar boundary layers in coarse grids. Annual Research Briefs, Center for Turbulence Research, Stanford University, 85-95.

Pressure Gradient Boundary Layer

- To test the FSWM in a more general setting, we applied it to flow over a flat plate with a spatially varying edge pressure gradient.
  - Assess the validity of the local self-similarity assumption for a more general flow



- $N_n = 5 \times N_s = 150$
  - Entirely subgrid laminar boundary layer

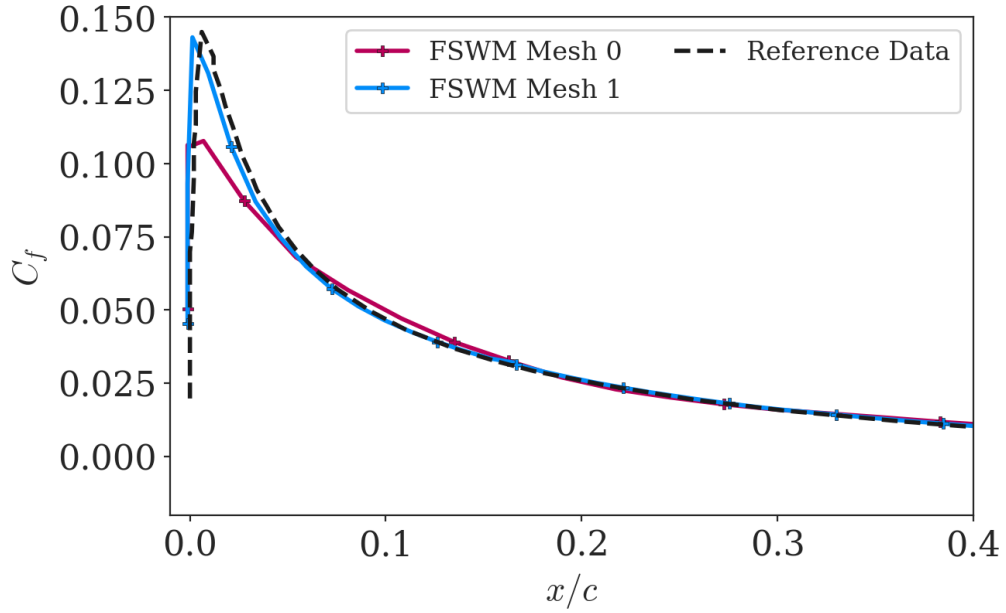


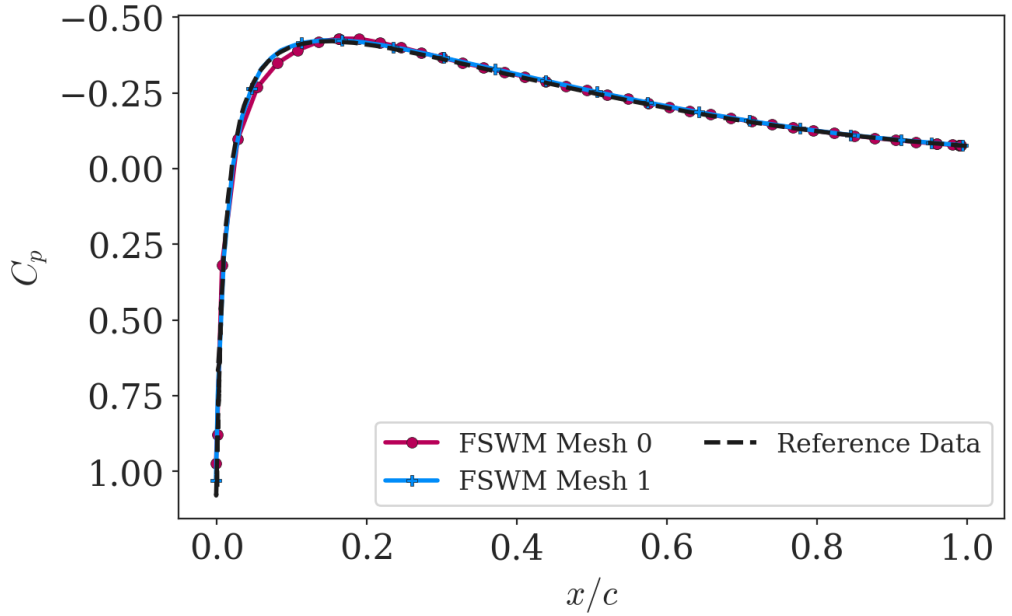
Gonzalez, C. A., Karp, M., & Moin, P. (2020). Wall-stress modeling for laminar boundary layers in coarse grids. Annual Research Briefs, Center for Turbulence Research, Stanford University, 85-95.

NACA0012 Airfoil

- Simulation parameters
  - $Re_c = 5000, Ma = 0.5, \alpha = 0°$

- Mesh 0: $\frac{\delta_{99}}{\Delta_y} = 4$ at 10% of chord
- Mesh 1: $\frac{\delta_{99}}{\Delta_y} = 10$ at 10% of chord





Swanson, R. C., & Langer, S. (2016). Steady-state laminar flow solutions for NACA 0012 airfoil. Computers & Fluids, 126, 102-128.

Overview



Laminar | Transitional | Turbulent

(1) Development of Falkner-Skan Wall Model

(2) Transition modeling with nonlinear parabolized stability equations

(3) Constructing WMLES inflow conditions from NLPSE

(4) Fully integrated PSE-Sponge simulations of transitional flows

Nonlinear Parabolized Stability Equations

- The parabolized stability equations are a reduced order model for the spatial evolution of disturbances
  - Shown to agree well with direct numerical simulations at a fraction of the cost
  - Suitable for the simulation of spatially varying, non-parallel baseflows
  - Physics based equations
  - The ability to model nonlinear effects make them a higher fidelity model

- The nonlinear PSE have been successfully applied to
  - High-amplitude disturbance flat plate simulations
  - Görtler vortex formation on concave surfaces
  - Swept wing vortex formation
  - High Mach cone simulations

Bertolotti, F. P., Herbert, T., & Spalart, P. R. (1992). Linear and nonlinear stability of the Blasius boundary layer. Journal of fluid mechanics, 242, 441-474.

Li, F., & Malik, M. R. (1995). Fundamental and subharmonic secondary instabilities of Görtler vortices. Journal of Fluid Mechanics, 297, 77-100.

Haynes, T. S., & Reed, H. L. (2000). Simulation of swept-wing vortices using nonlinear parabolized stability equations. *Journal of Fluid Mechanics*, *405*, 325-349.

Paredes, P., Choudhari, M. M., Li, F., Jewell, J. S., & Kimmel, R. L. (2019). Nonmodal growth of traveling waves on blunt cones at hypersonic speeds. *AIAA Journal*, *57*(11), 4738-4749.

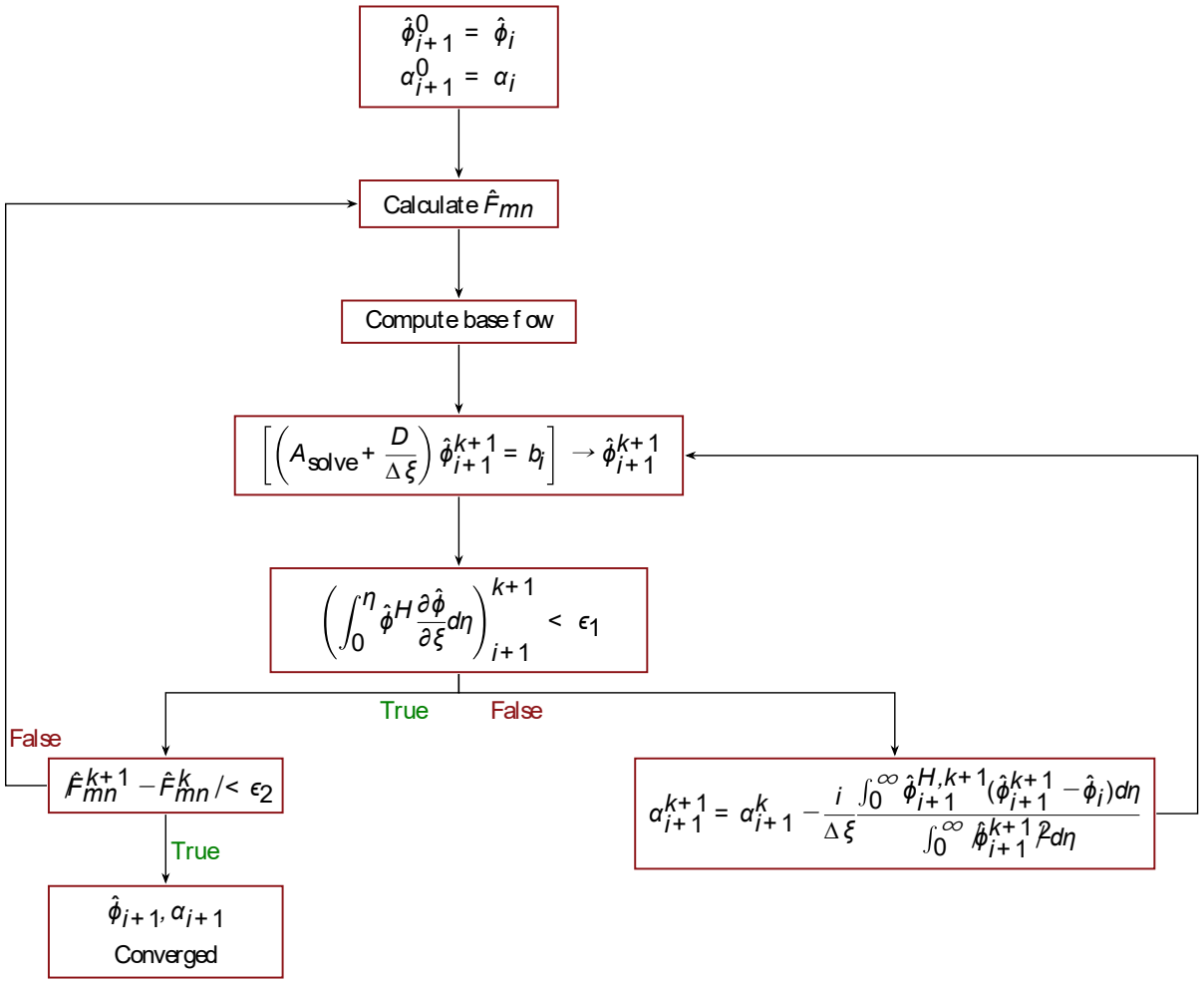
Nonlinear Parabolized Stability Equations In Curvilinear Coordinates

- The PSE assumption is that we can decompose disturbances into a **slowly varying amplitude function**, and a **fast oscillatory part**

$$\phi'(\xi,\eta,z,t) = \sum_{n=-N}^{N}\sum_{m=-M}^{M} \hat{\phi}_{mn}(\xi,\eta)\exp\left(i\int_{\xi_0}^{\xi}\alpha_{mn}(\xi')d\xi' + in\beta z - im\omega t\right)$$

$$A\hat{\phi}_{m,n} + B\frac{\partial\hat{\phi}_{m,n}}{\partial\eta} + C\frac{\partial^2\hat{\phi}_{m,n}}{\partial\eta^2} + D\frac{\partial\hat{\phi}_{m,n}}{\partial\xi} + E\frac{\partial\hat{\phi}_{m,n}}{\partial z} + G\frac{\partial^2\hat{\phi}_{m,n}}{\partial z^2} + H\frac{\partial^2\hat{\phi}}{\partial\xi\partial\eta} = \hat{F}_{m,n}$$

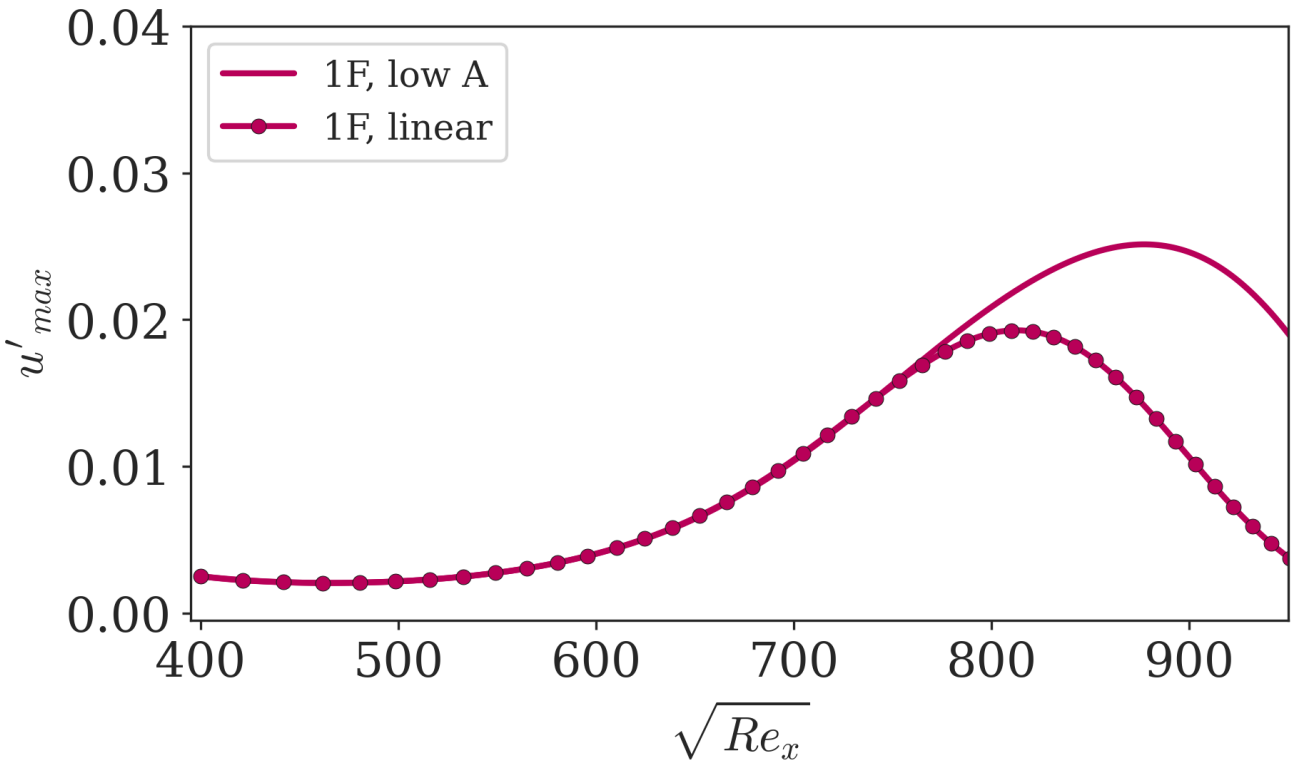
- Cost savings from:
  - Truncation of the series representation for disturbances
  - Coarse streamwise grid only needs to resolve the amplitude function
  - Wave ansatz in the spanwise direction



Herbert, T. (1997). Parabolized stability equations. Annual Review of Fluid Mechanics, 29(1), 245-283.

Nonlinear Transition Effects

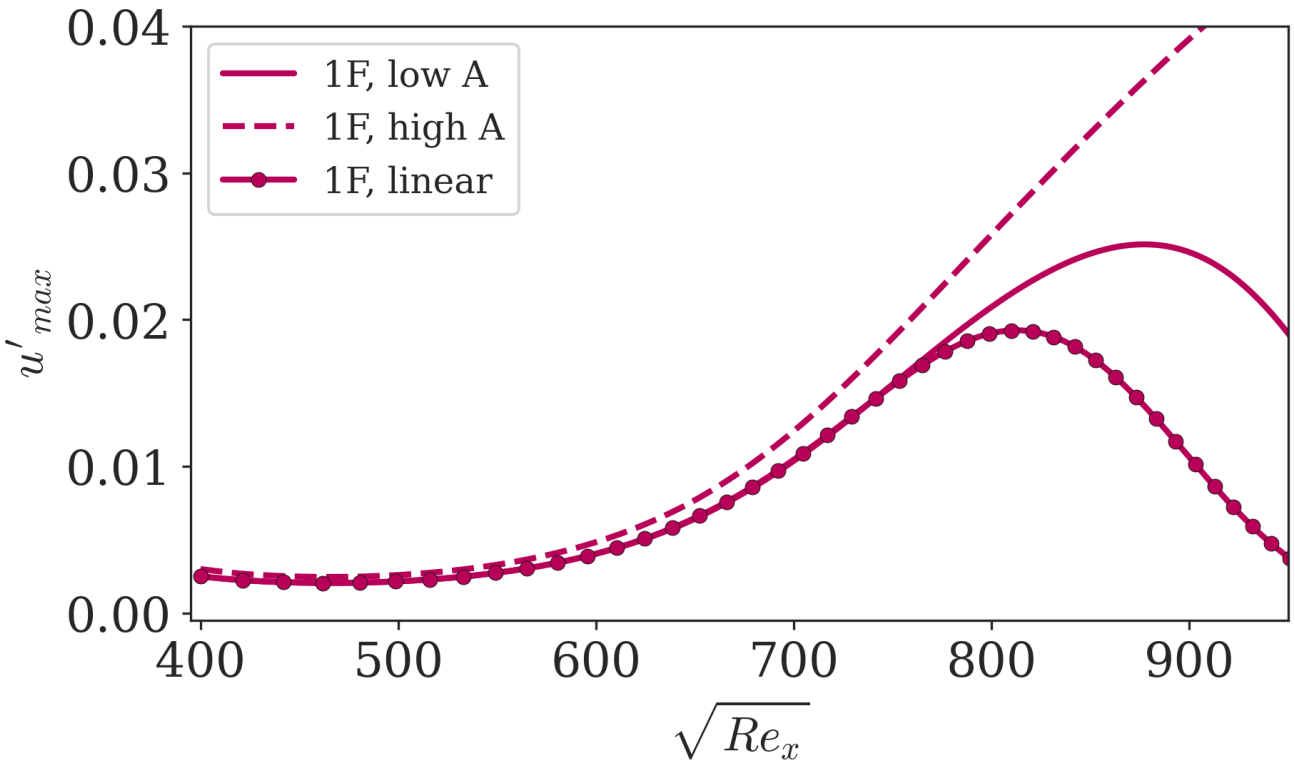
- TS mode propagation over a zero pressure gradient flat plate boundary layer
- Nonlinear PSE predicts higher amplitude growth



Bertolotti, F. P., Herbert, T., & Spalart, P. R. (1992). Linear and nonlinear stability of the Blasius boundary layer. Journal of fluid mechanics, 242, 441-474.

Nonlinear Transition Effects

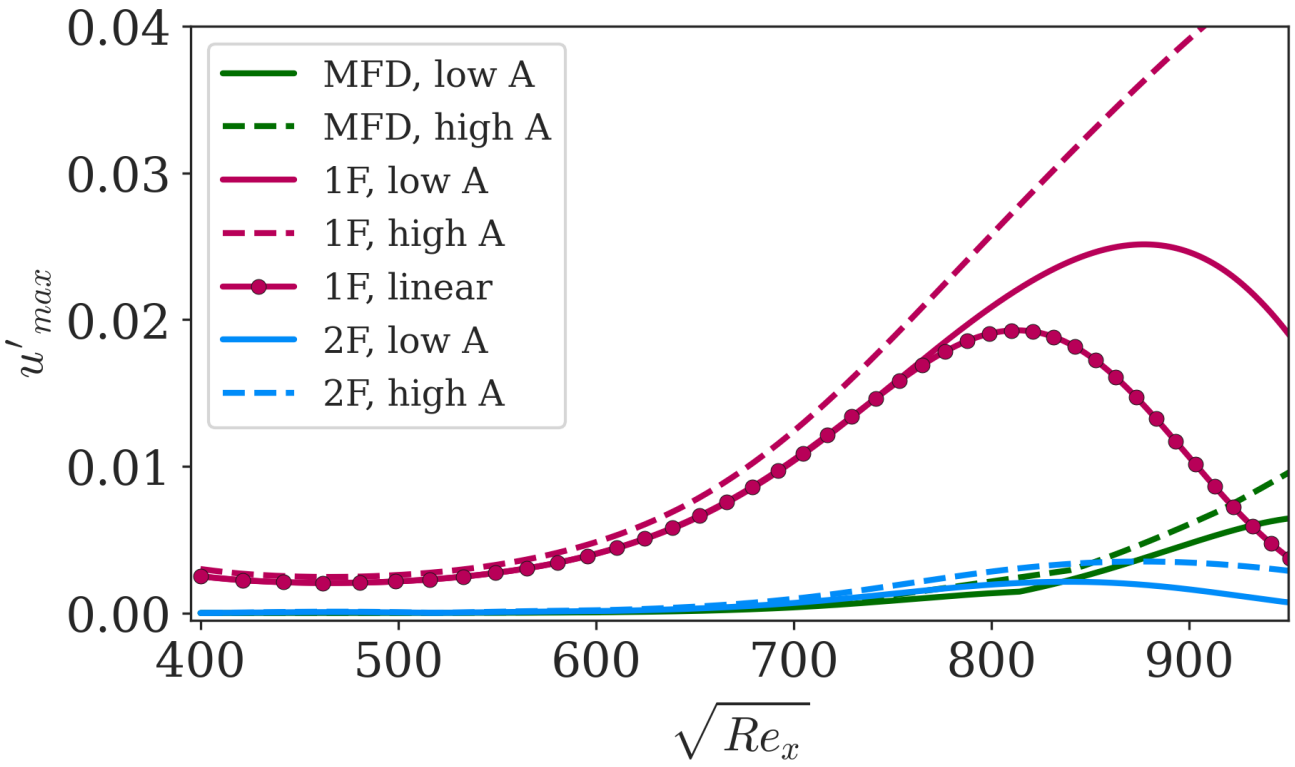
- TS mode propagation over a zero pressure gradient flat plate boundary layer
- Nonlinear PSE predicts higher amplitude growth
- Nonlinear PSE accounts for initial conditions
  - Linear PSE only provides a solution unique up to a constant coefficient scaling



Bertolotti, F. P., Herbert, T., & Spalart, P. R. (1992). Linear and nonlinear stability of the Blasius boundary layer. Journal of fluid mechanics, 242, 441-474.

Nonlinear Transition Effects

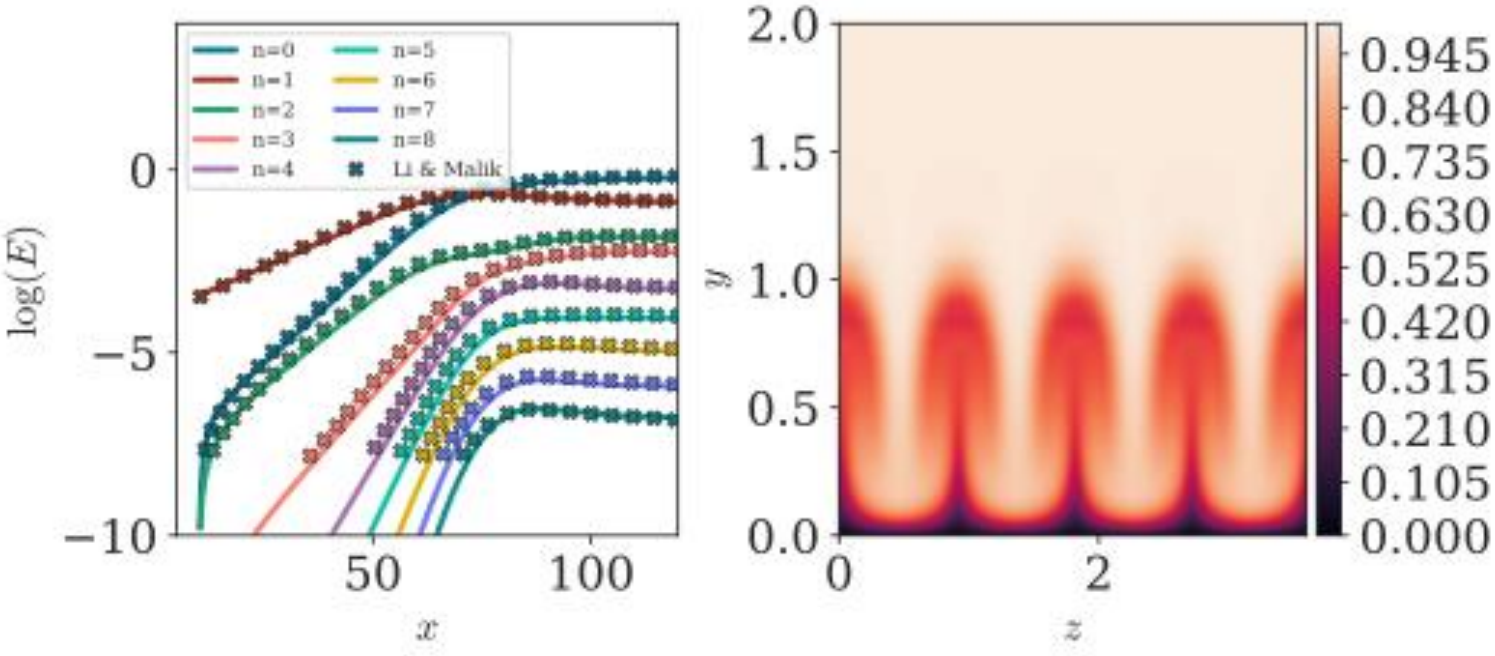
- TS mode propagation over a zero pressure gradient flat plate boundary layer
- Nonlinear PSE predicts higher amplitude growth
- Nonlinear PSE accounts for initial conditions
  - Linear PSE only provides a solution unique up to a constant coefficient scaling
- Nonlinear PSE predicts the evolution of higher harmonic disturbances in the flow and mean flow distortion (MFD)



Bertolotti, F. P., Herbert, T., & Spalart, P. R. (1992). Linear and nonlinear stability of the Blasius boundary layer. Journal of fluid mechanics, 242, 441-474.

NLPSE Solver

- General stability code that can solve
  - › Orr-Sommerfeld
  - › Görtler
  - › LPSE
  - › NLPSE
- Parallelized with mpi4py
- 4th order finite differences in the wall-normal direction
- Backward Euler in streamwise direction
- Supports body-fitted curvilinear grids
- Verification cases
  - › TS mode propagation
  - › Subharmonic mode propagation
  - › Oblique mode propagation
  - › Görtler vortex formation
  - › Airfoil stability analysis



Joslin, R. D., et al. (1993). Spatial direct numerical simulation of boundary-layer transition mechanisms: Validation of PSE theory. Theoretical and Computational Fluid Dynamics, 4(6), 271-288.

Bertolotti, F. P., Herbert, T., & Spalart, P. R. (1992). Linear and nonlinear stability of the Blasius boundary layer. Journal of fluid mechanics, 242, 441-474.

Li, F., & Malik, M. R. (1995). Fundamental and subharmonic secondary instabilities of Görtler vortices. Journal of Fluid Mechanics, 297, 77-100.

Gonzalez, C. A., Harris, S. R., & Moin, P. glimPSE: an open-source incompressible nonlinear parabolized stability equation solver.

Overview



(1) Development of Falkner-Skan Wall Model

(2) Transition modeling with nonlinear parabolized stability equations

(3) Constructing WMLES inflow conditions from NLPSE

(4) Fully integrated PSE-Sponge simulations of transitional flows

LES solver charLES

- We use the flow solver charLES for all LES simulations
  - Developed by Cascade Technologies / Cadence
- Massively parallel, finite volume, compressible solver
- 2nd order low dissipation spatial discretization
  - Suitable for arbitrary unstructured, polyhedral Voronoi meshes
- Explicitly marched 3rd order Runge-Kutta
- We utilize the dynamic Smagorinsky subgrid scale model
  - Automatically goes to zero in laminar and transitional regions of flow[1]

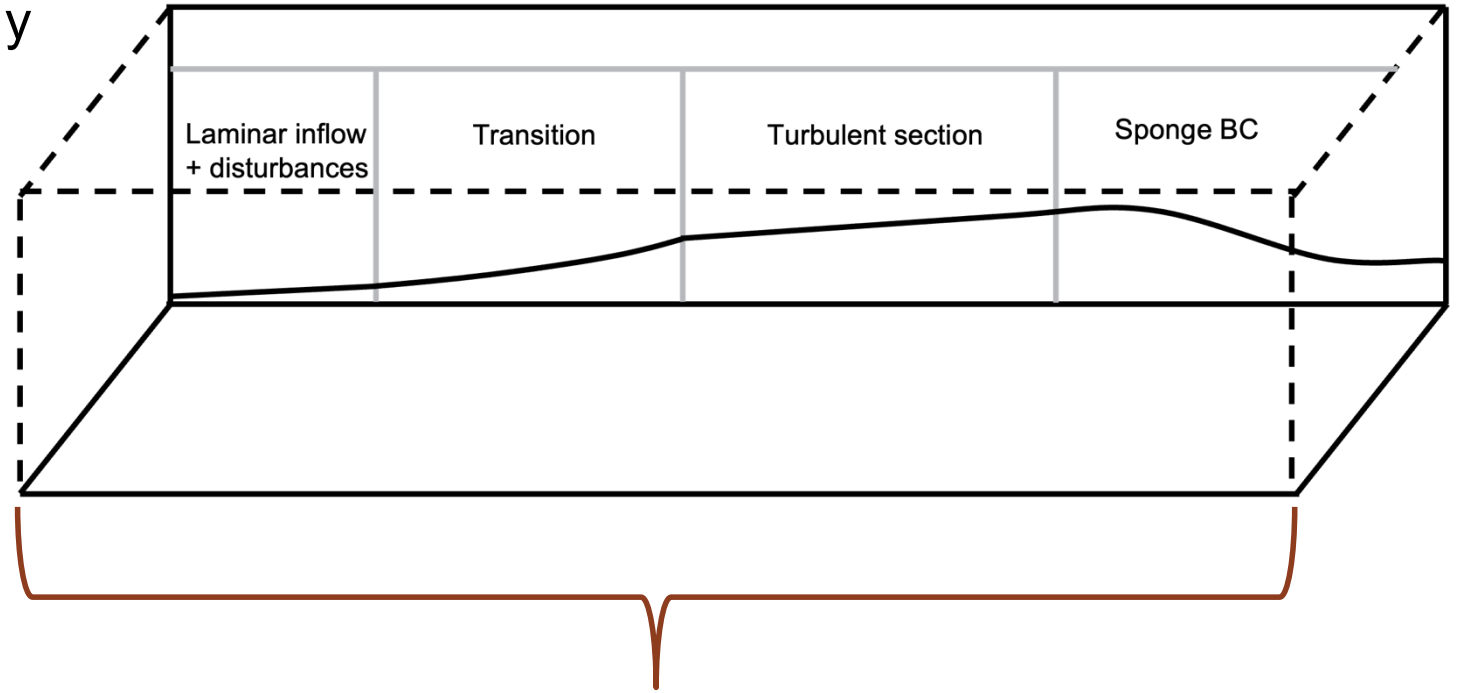
[1] Sayadi, T., & Moin, P. (2012). Large eddy simulation of controlled transition to turbulence. *Physics of Fluids*, *24*(11).

Model Problem

- We are interested in simulating a naturally transitioning zero pressure gradient flat plate boundary layers

- Computational domain
  - $L_x = 350\delta_{99}, L_y = 30\delta_{99}, L_z = 20\delta_{99}$

Standard Approach



Ham, F., Mattsson, K., & Iaccarino, G. (2006). Accurate and stable finite volume operators for unstructured flow solvers. Annual Research Briefs, 243-261.

Herbert, T. (1991, January). Boundary-layer transition-analysis and prediction revisited. In 29th Aerospace Sciences Meeting (p. 737).

Joslin, R. D., Streett, C. L., & Chang, C. L. (1993). Spatial direct numerical simulation of boundary-layer transition mechanisms: Validation of PSE theory. Theoretical and Computational Fluid Dynamics, 4(6), 271-288.

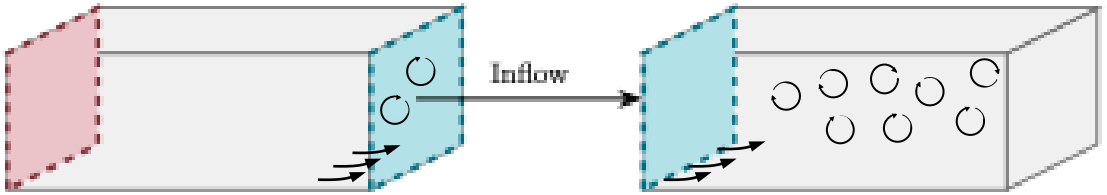
Modeling Approach

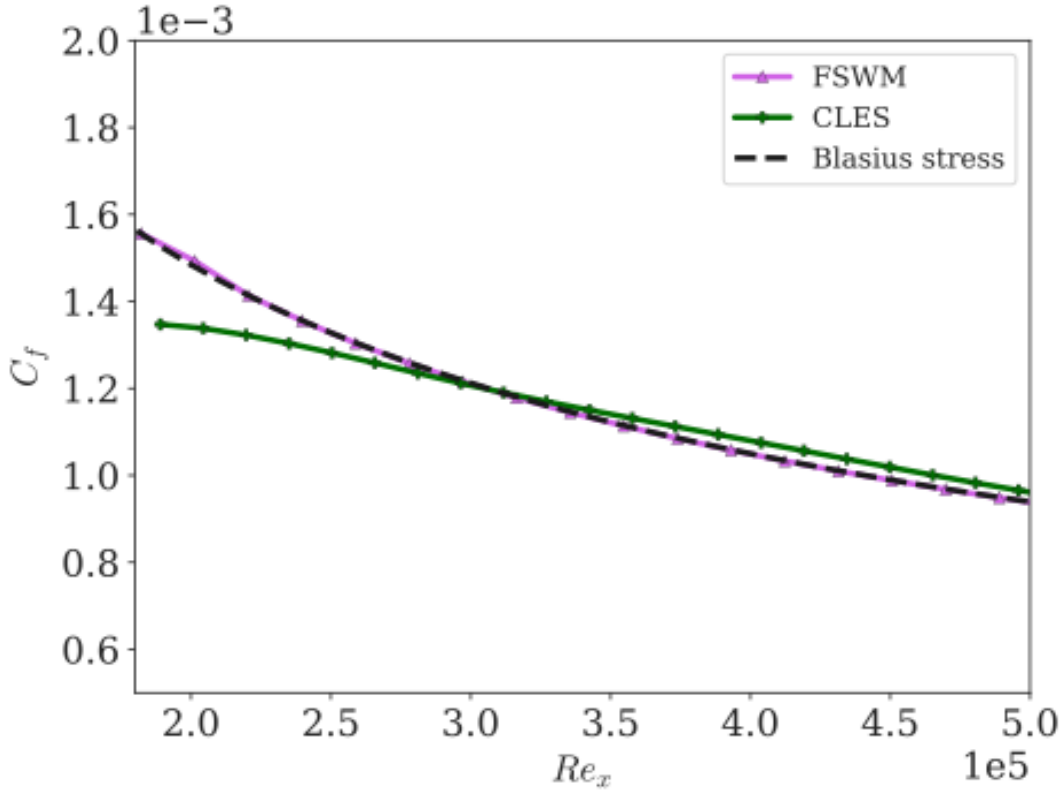
1. Precursor simulation using the FSWM.



2. Nonlinear marching to the point of transition.

3. Turbulent equilibrium wall model is valid everywhere within this domain.





Lozano-Durán, A., Hack, M. J. P., & Moin, P. (2018). Modeling boundary-layer transition in direct and large-eddy simulations using parabolized stability equations. Physical review fluids, 3(2), 023901.

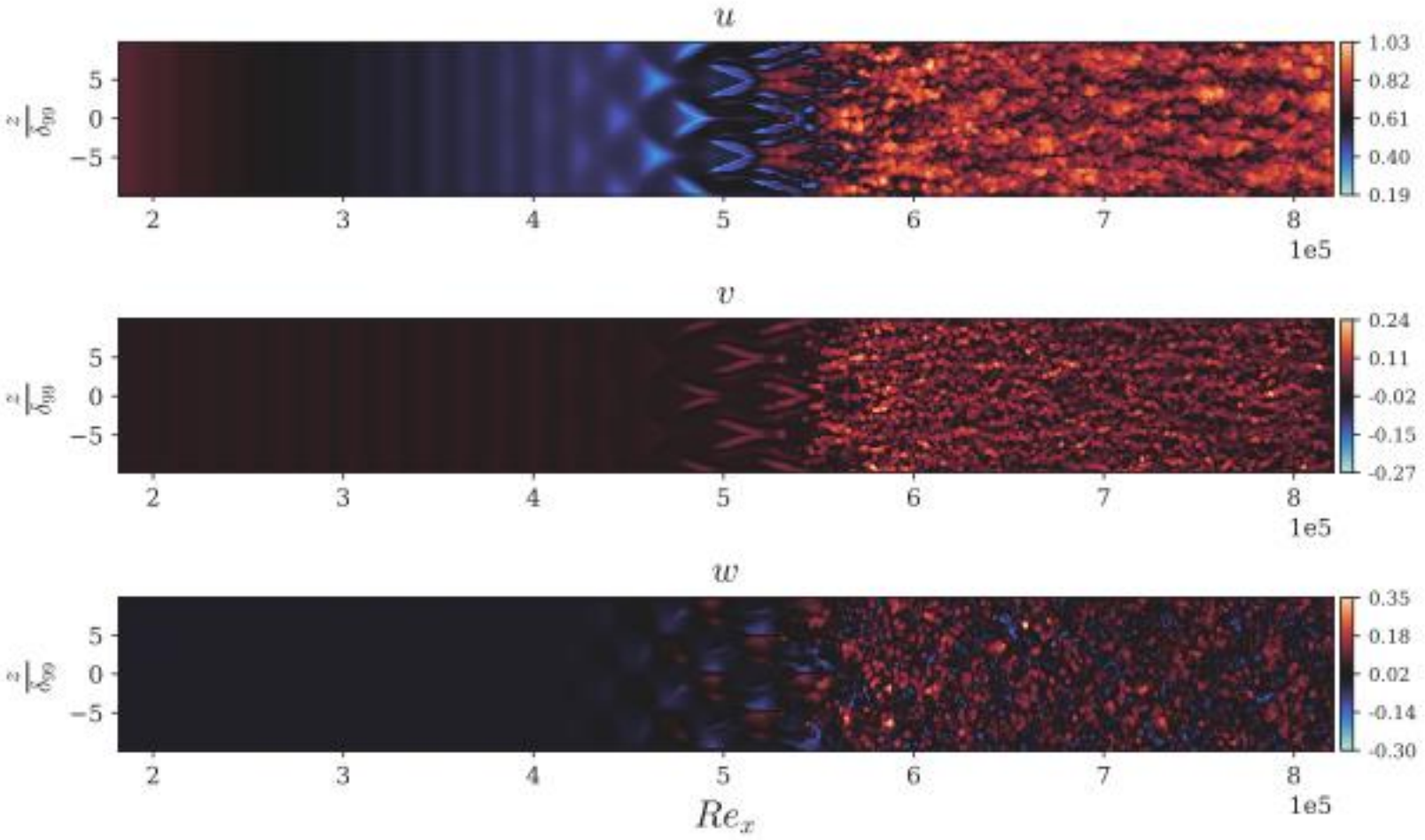
Gonzalez, C. A., Harris, S. R., & Moin, P. (2021). Falkner-Skan wall model baseflow generation for the parabolized stability equations. Annual Research Briefs, Center for Turbulence Research, Stanford University, 73-81.

DNS of H-type Transitioning Boundary Layer

- $Re_x = 1.8 \cdot 10^5$ at the inlet

- Mesh details
  - $N_x = 5000, N_y = 400, N_z = 400$
  - $\Delta x^+ = 6.8, \Delta y^+ = 0.49, \Delta z^+ = 5.6$
  - $N = 800 \cdot 10^6$

- Inflow disturbances
  - $F = \frac{\omega\nu}{U_\infty^2} \cdot 10^6 = 124$
  - $b = \frac{\beta\nu}{U_\infty} \cdot 10^3 = \pm 0.3303$
  - $A_{TS} = 0.0048$
  - $A_{SH} = 0.145 \cdot 10^{-4}$

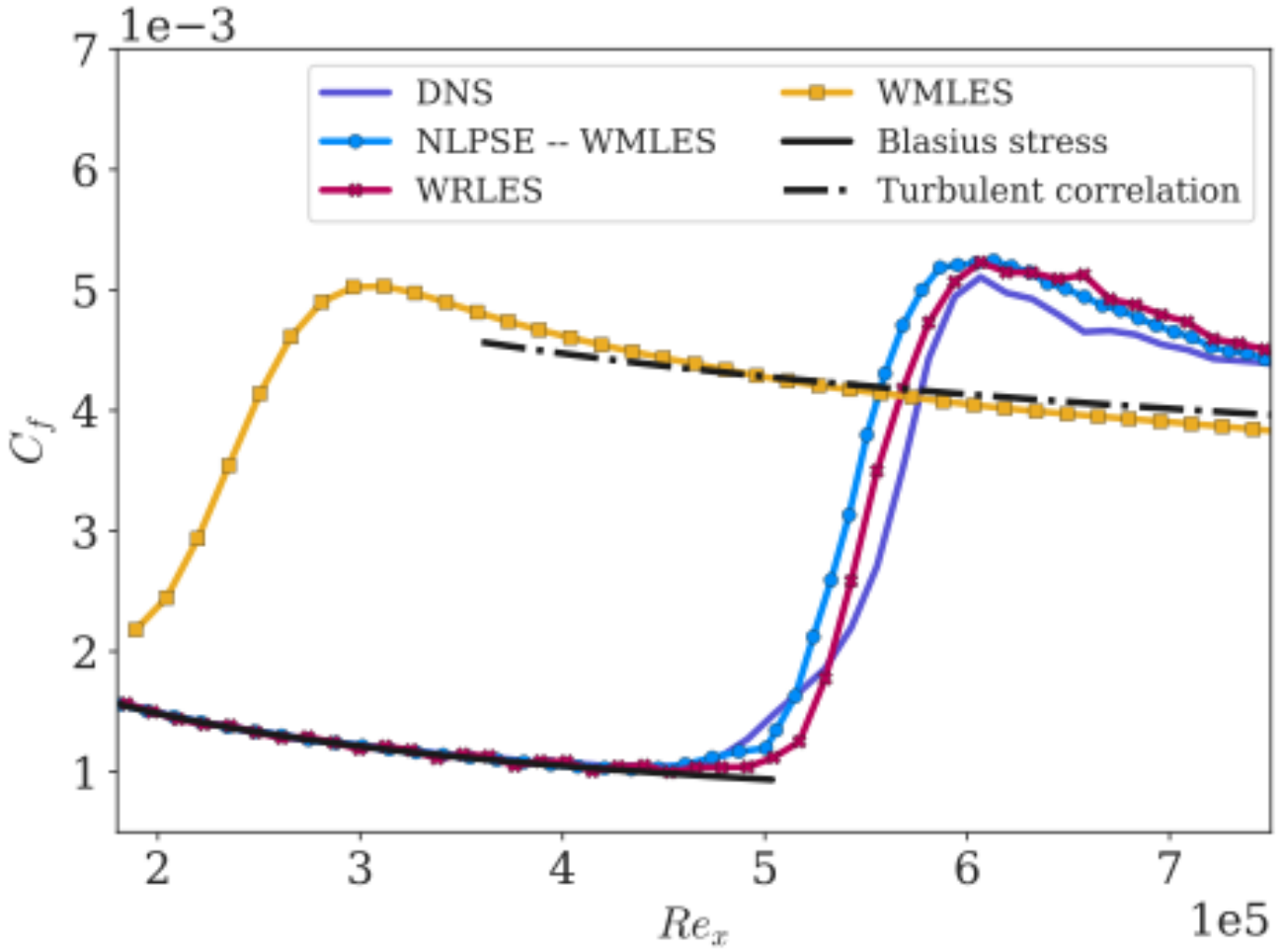


Joslin, R. D., et al. (1993). Spatial direct numerical simulation of boundary-layer transition mechanisms: Validation of PSE theory. Theoretical and Computational Fluid Dynamics, 4(6), 271-288.

Gonzalez, C. A., Harris, S. R., & Moin, P. (2021). Falkner-Skan wall model baseflow generation for the parabolized stability equations. Annual Research Briefs, Center for Turbulence Research, Stanford University, 73-81.

H-type Skin Friction Comparison

- WRLES predicts the transition location and overall skin-friction curve well
  - Cost is lower than DNS, but out of reach for practical simulations
- Standard WMLES mispredicts the entire flow field
  - Transitions near the inlet
- NLPSE generated inflow for WMLES accurately predicts the transition location, skin-friction overshoot, and the decay to the turbulent correlation



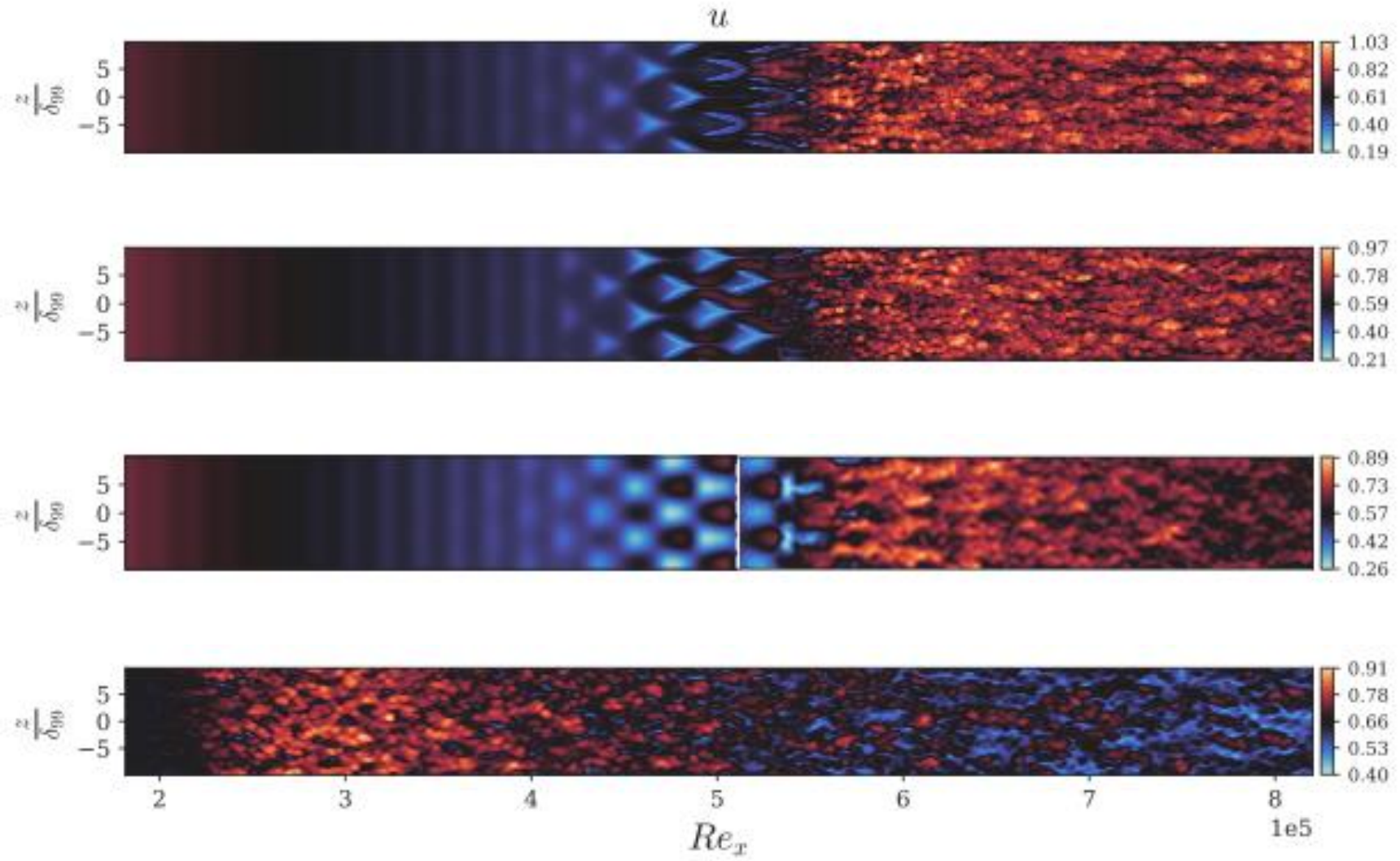
H-type Transition Flow Structures

DNS

WRLES

NLPSE—WMLES

WMLES



H-type Transition Computational Cost Comparison

- NLPSE—WMLES approach results in a **99% reduction** in cell count compared to DNS and a **98% reduction** compared to WRLES
- NLPSE — WMLES approach offers a **250x** cost reduction to accurately simulate this case

	N_x	N_y	N_z	N_{cv}
DNS	5000	400	400	$8.0E8$
WRLES	1100	300	200	$6.6E7$
WMLES	650	60	80	$3.12E6$
NLPSE–WMLES	250	100	1	$2.5E4$
	380	60	40	$9.12E5$

Gonzalez, C. A., Harris, S. R., & Moin, P. (2023). Simulating an H-type transitional boundary layer in a coupled NLPSE and WMLES framework with a Falkner-Skan wall model. Annual Research Briefs, Center for Turbulence Research, Stanford University, 307-320.

Towards complex geometry

- Cutting computational domains to use the PSE-Inflow approach can be cumbersome on complex geometries

- A novel approach has been developed to overcome this limitation using sponges

- Benefits
  - Unstructured grids
  - Asymmetric transition fronts
  - Complex geometry
  - Does not require splitting the computational domain

- First verified on canonical flat plate transition

Overview



Laminar

Transitional

Turbulent

(1) Development of Falkner-Skan Wall Model

(2) Transition modeling with nonlinear parabolized stability equations

(3) Constructing WMLES inflow conditions from NLPSE

(4) Fully integrated PSE-Sponge simulations of transitional flows

PSE-Sponge Method

- In this method, the LES equations are modified to include a forcing parameter on the RHS that corrects the LES solution toward the more accurate NLPSE solution

$$\frac{\partial \overline{\rho}}{\partial t} + \frac{\partial \overline{\rho}\,\tilde{u}_j}{\partial x_j} = \sigma^*(\overline{\rho}_{PSE} - \overline{\rho})$$

$$\frac{\partial \overline{\rho}\,\tilde{u}_j}{\partial t} + \frac{\partial \overline{\rho}\,\tilde{u}_i\tilde{u}_j}{\partial x_j} + \frac{\partial \overline{p}}{\partial x_i} - \frac{\partial \tilde{\tau}_{ij}}{\partial x_j} + \frac{\partial \tau_{ij}^{sgs}}{\partial x_j} = \sigma^*\left((\overline{\rho}\,\tilde{u}_j)_{PSE} - \overline{\rho}\,\tilde{u}_j\right)$$

$$\frac{\partial \overline{E}}{\partial t} + \frac{\partial\left[\left(\overline{E}+\overline{p}\right)\tilde{u}_j\right]}{\partial x_j} - \frac{\partial(\tilde{u}_i\tilde{\tau}_{ij})}{\partial x_j} + \frac{\partial\left(\tilde{u}_i\tau_{ij}^{sgs}\right)}{\partial x_j} - \frac{\partial}{\partial x_j}\left(k\frac{\partial \overline{T}}{\partial x_j}\right) + \frac{\partial Q_j^{sgs}}{\partial x_j} = \sigma^*(\overline{E}_{PSE} - \overline{E})$$

- We also impose the PSE computed shear stress as the wall boundary condition which accounts for mean flow distortion

$$\tau_{w,LES} = \tau_{w,PSE}$$

PSE-Sponge Method

- In this method, the LES equations are modified to include a forcing parameter on the RHS that corrects the LES solution toward the more accurate NLPSE solution

$$\frac{\partial \overline{\rho}}{\partial t} + \frac{\partial \overline{\rho}\,\tilde{u}_j}{\partial x_j} = \cancel{0}\;\sigma^*(\overline{\rho}_{PSE} - \overline{\rho})$$

$$\frac{\partial \overline{\rho}\,\tilde{u}_j}{\partial t} + \frac{\partial \overline{\rho}\,\tilde{u}_i\tilde{u}_j}{\partial x_j} + \frac{\partial \overline{p}}{\partial x_i} - \frac{\partial \tilde{\tau}_{ij}}{\partial x_j} + \frac{\partial \tau_{ij}^{sgs}}{\partial x_j} = \sigma^*\left((\overline{\rho}\,\tilde{u}_j)_{PSE} - \overline{\rho}\,\tilde{u}_j\right)$$

$$\frac{\partial \overline{E}}{\partial t} + \frac{\partial\left[\left(\overline{E}+\overline{p}\right)\tilde{u}_j\right]}{\partial x_j} - \frac{\partial(\tilde{u}_i\tilde{\tau}_{ij})}{\partial x_j} + \frac{\partial\left(\tilde{u}_i\tau_{ij}^{sgs}\right)}{\partial x_j} - \frac{\partial}{\partial x_j}\left(k\frac{\partial \overline{T}}{\partial x_j}\right) + \frac{\partial Q_j^{sgs}}{\partial x_j} = \cancel{0}\;\sigma^*(\overline{E}_{PSE} - \overline{E})$$

- We also impose the PSE computed shear stress as the wall boundary condition which accounts for mean flow distortion

$$\tau_{w,LES} = \tau_{w,PSE}$$

PSE-Sponge Method

- σ^* is an inverse time scale subject to

$$\Delta t \leq \frac{1}{\sigma^*} \leq t_{TS}$$

- We define

$$\sigma = \sigma^* t_{TS} = \frac{2\pi\sigma^*}{\omega_{TS}}$$

and enforce $\sigma \neq 0$ in the volume where the PSE equations are valid

- A blending function is used to smoothly switch between regions of zero forcing and nonzero forcing

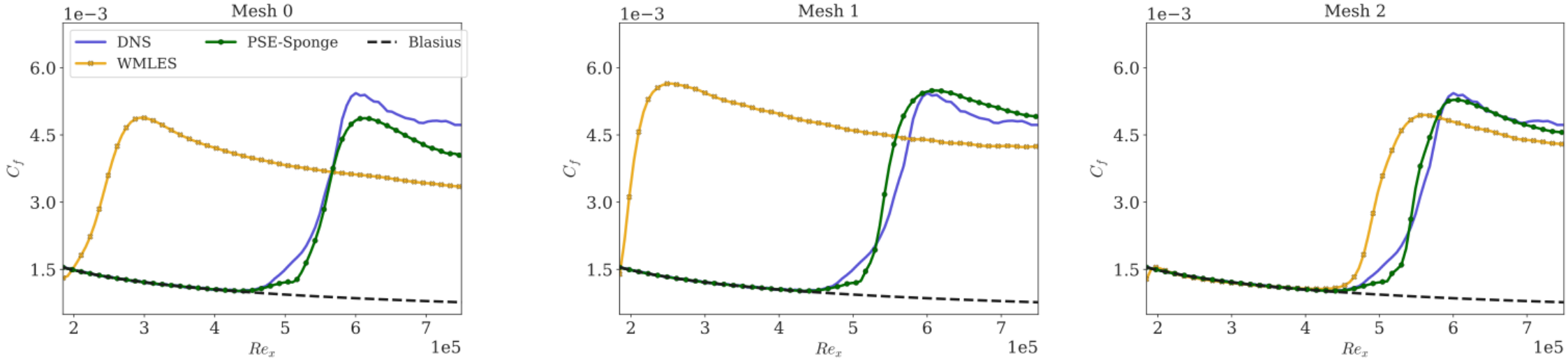
$$\gamma = 0.5\left(1 + \tanh\left(\frac{(x - x_{tr})\alpha_{TS}}{2\pi}\right)\right)$$

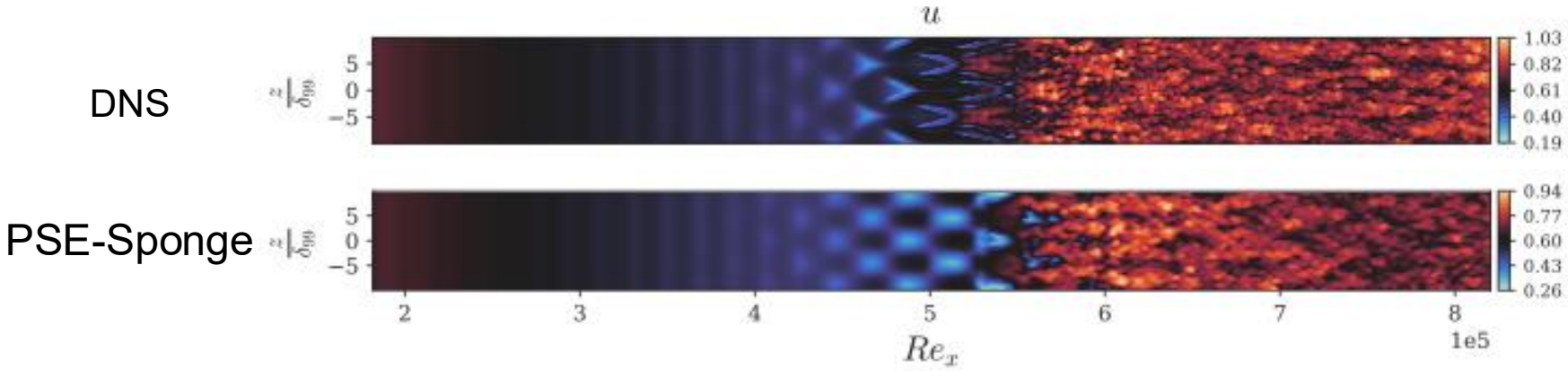
H-type Transition using PSE-Sponge

- Across all grids simulated, PSE-Sponge method outperforms WMLES

	$\frac{\lambda_x}{\Delta x}$	$\frac{\delta_{99}}{\Delta y}$	$\frac{\lambda_z}{\Delta z}$	N_{cv}
Mesh 0	18	4	36	$3.12E6$
Mesh 1	18	8	36	$6.2E6$
Mesh 2	37	8	73	$2.5E7$

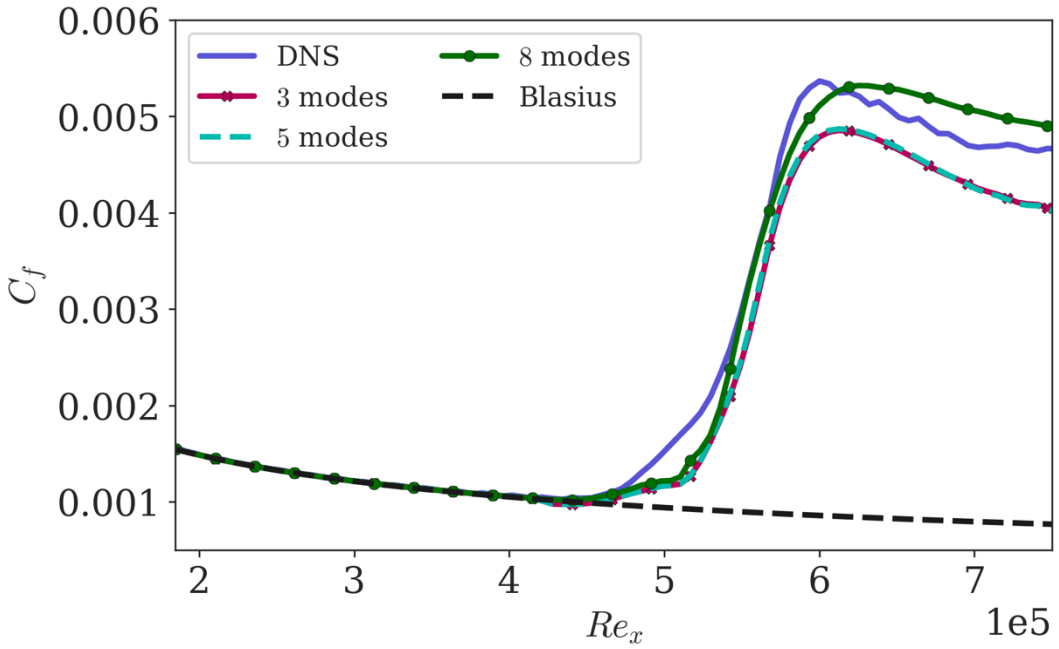
- PSE-Sponge simulations save 2 orders of magnitude computational cells compared to DNS





PSE-Sponge Sensitivity

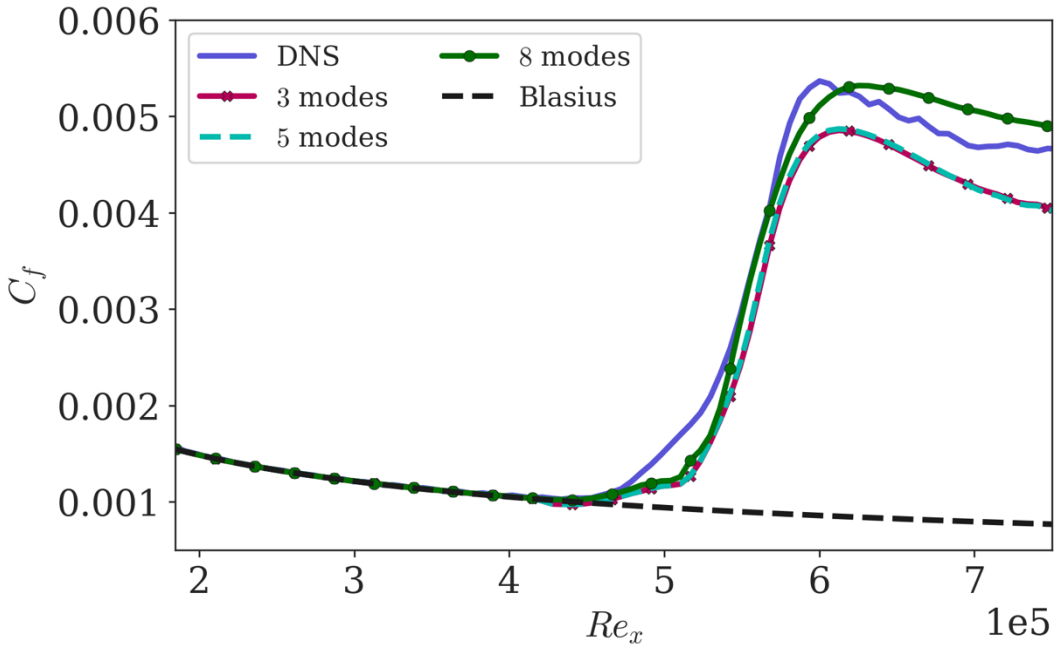
- Sensitivity to the quantity of modes in the sponge layer is observed
  - Higher harmonics have smaller scales and therefore require a finer LES grid

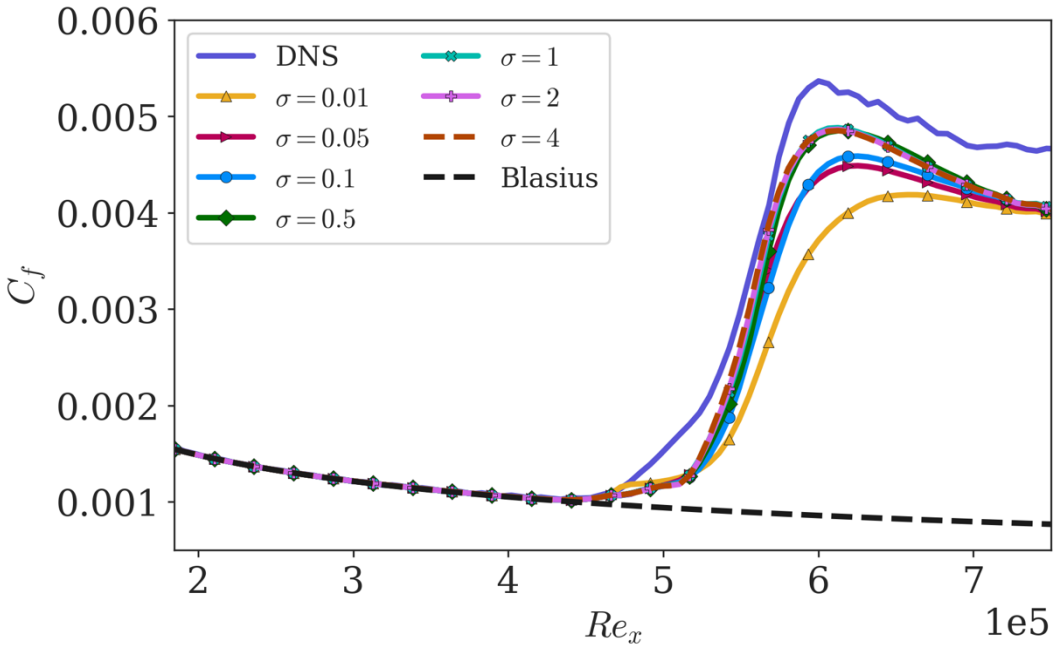


PSE-Sponge Sensitivity

- Sensitivity to the quantity of modes in the sponge layer is observed
  - Higher harmonics have smaller scales and therefore require a finer LES grid

- Small values of the sponge parameter reduce the magnitude of volumetric forcing and therefore the LES is farther from the more accurate PSE state
  - The variation in σ displays smooth changes in the skin-friction prediction and convergence on this parameter is achieved at $\sigma = 0.5$ for this case

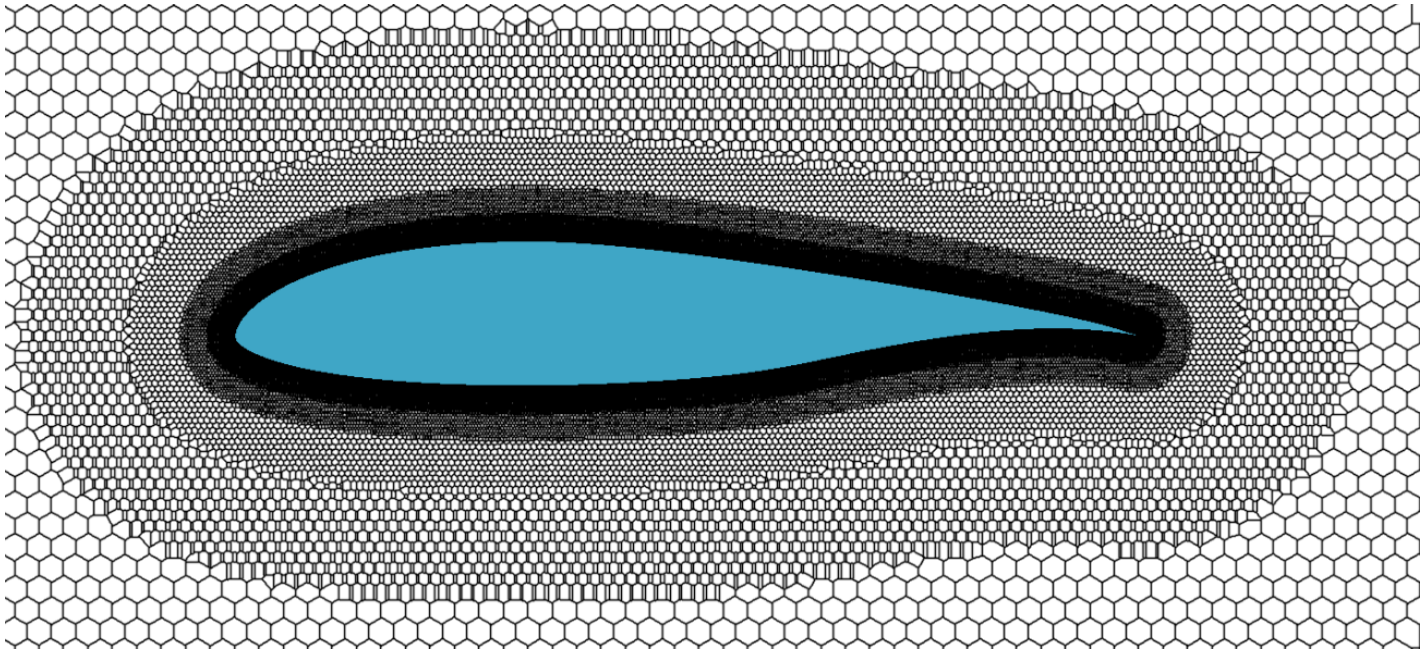




Natural Laminar Flow Airfoil Background

- The NLF(01)-0416 airfoil is a natural laminar flow configuration that was developed at the NASA Langley Research Center[1]
  - At $\alpha = 0°$, transition is triggered by TS instabilities on the upper and lower surfaces of the airfoil[2]

- Case details
  - $Ma = 0.1$
  - $Re_c = 4 \cdot 10^6$
  - $\alpha = 0°$
  - $25c$ radius mesh

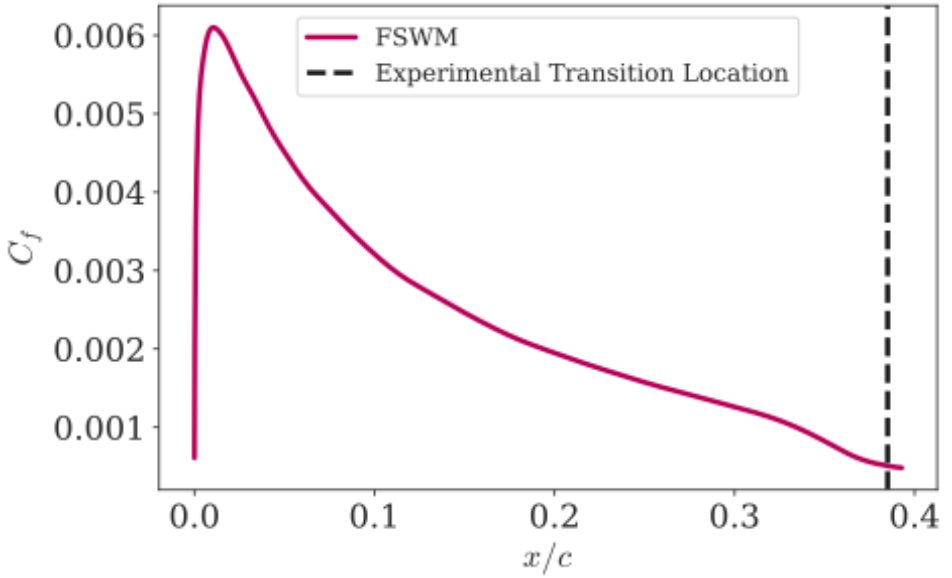


[1] Somers, D. M., "Design and Experimental Results for a Natural Laminar Flow Airfoil for General Aviation Applications," NASA TP-1861, June 1981, https://ntrs.nasa.gov/citations/19810015487.

[2] Shankar Venkatachari, B., Mysore, P. V., Hildebrand, N., Choudhari, M. M., & Denison, M. F. (2024). Verification of the γ-R e θ T Transition Model in OVERFLOW and FUN3D. Journal of Aircraft

NLF PSE-Sponge Setup

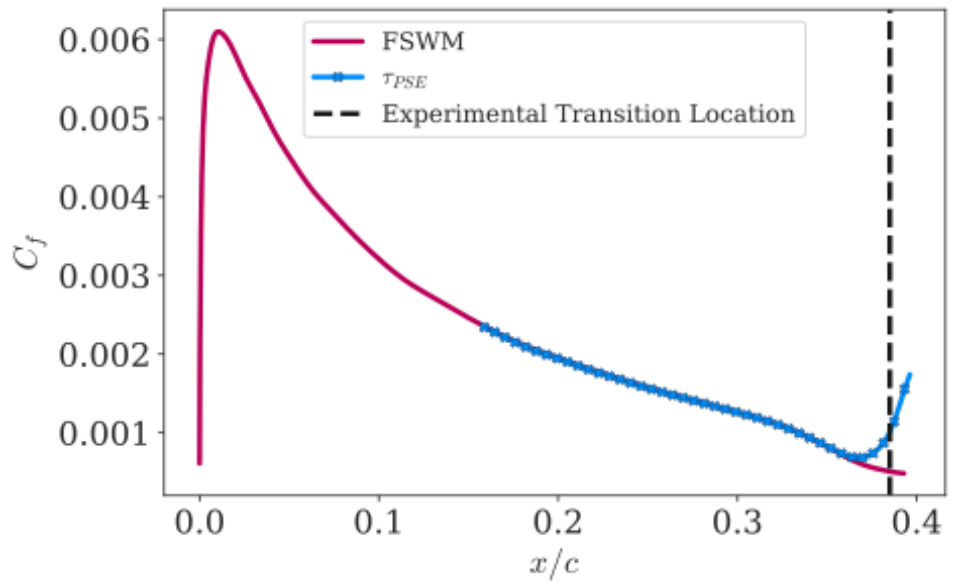
- Laminar FSWM precursor simulation of the NLF airfoil generate baseflows for NLPSE analysis

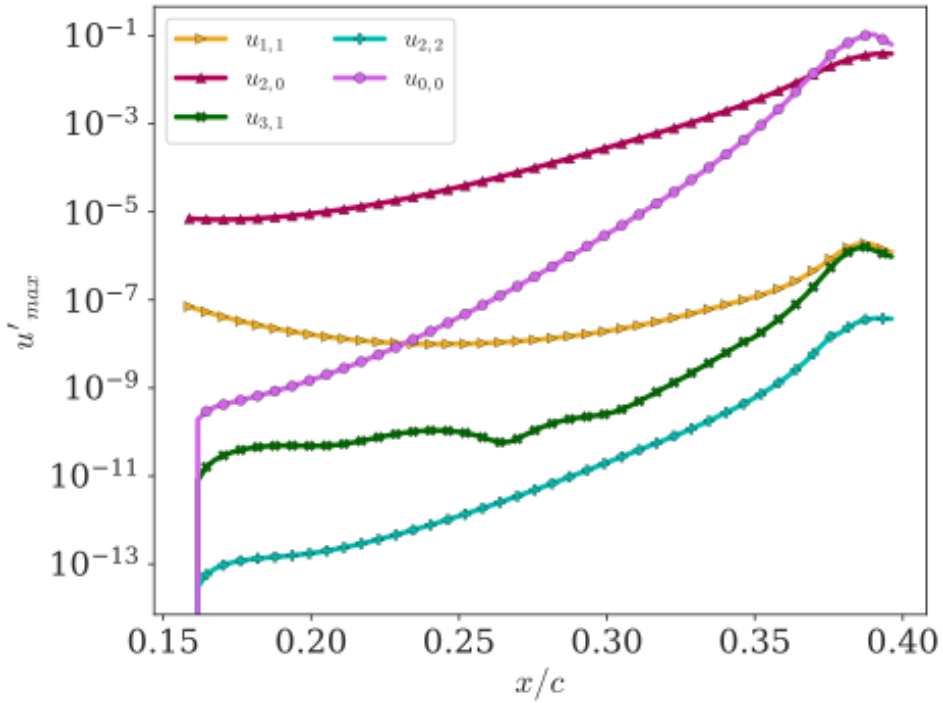


NLF PSE-Sponge Setup

- Laminar FSWM precursor simulation of the NLF airfoil generate baseflows for NLPSE analysis

- Because the disturbance environment of the experiment is not well characterized, we choose the NLPSE parameters to match the experimental transition location
  - H-type transition setup on the upper and lower sides of the airfoil
    - $F = 20, b = 0.02, \mathrm{A_{TS}} = 1\mathrm{E}-5, \mathrm{A_{SH}} = 1\mathrm{E}-7$



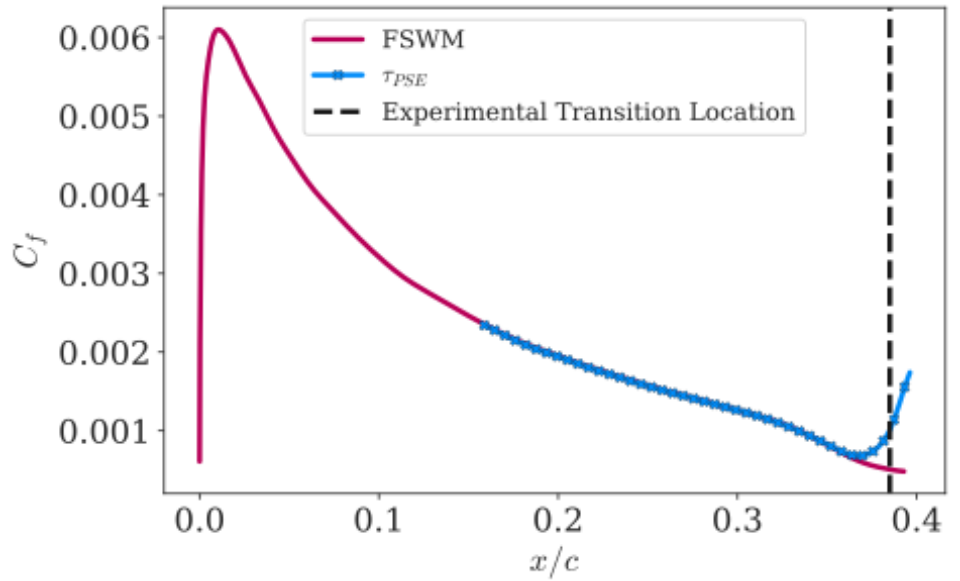


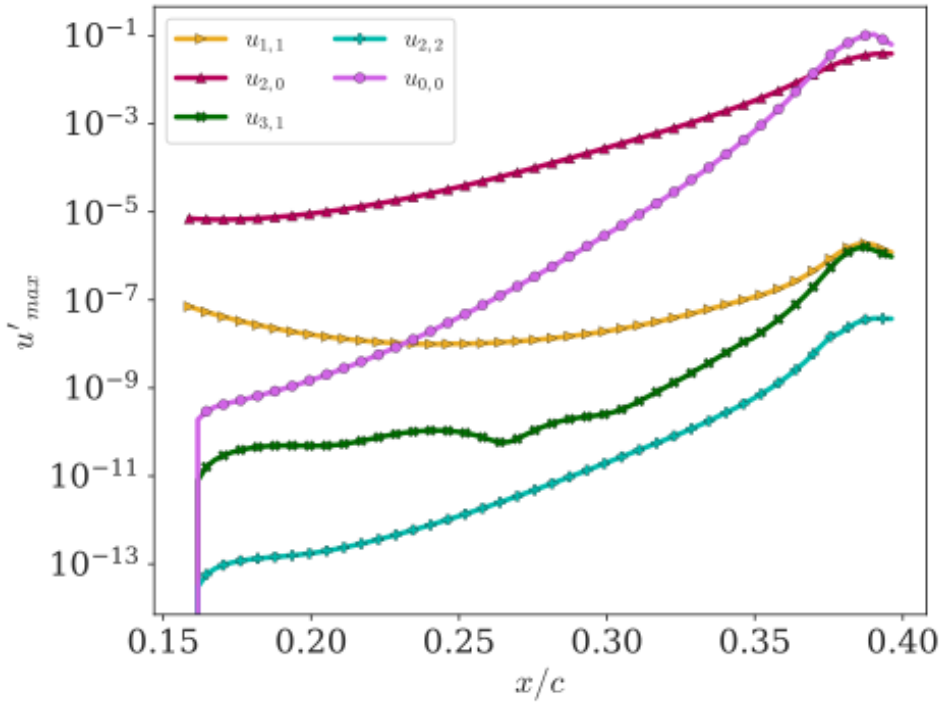
NLF PSE-Sponge Setup

- Laminar FSWM precursor simulation of the NLF airfoil generate baseflows for NLPSE analysis

- Because the disturbance environment of the experiment is not well characterized, we choose the NLPSE parameters to match the experimental transition location
  - H-type transition setup on the upper and lower sides of the airfoil
    - $F = 20, b = 0.02, \mathrm{A_{TS}} = 1\mathrm{E} - 5, \mathrm{A_{SH}} = 1\mathrm{E} - 7$

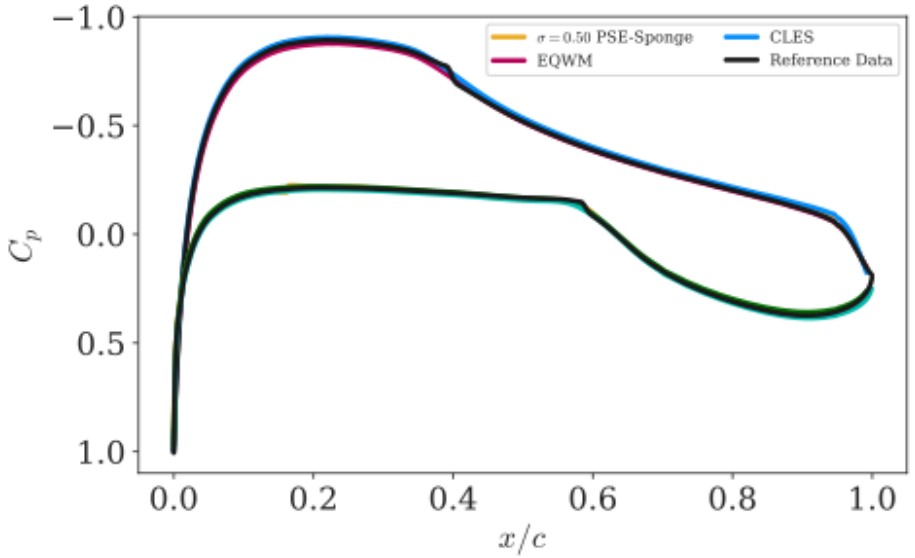
- Simulated PSE-Sponge, CLES, and EQWM on identical mesh
  - $\frac{\delta_{99}}{\Delta y} = 10$ at $\frac{x}{c} = 0.2$

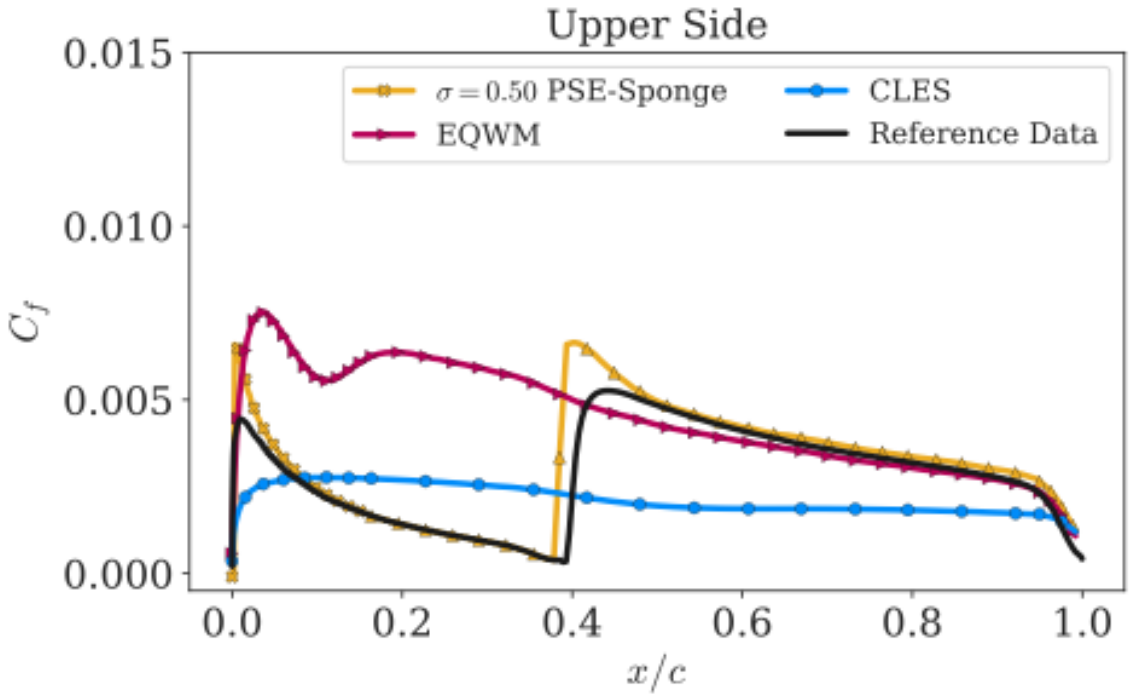


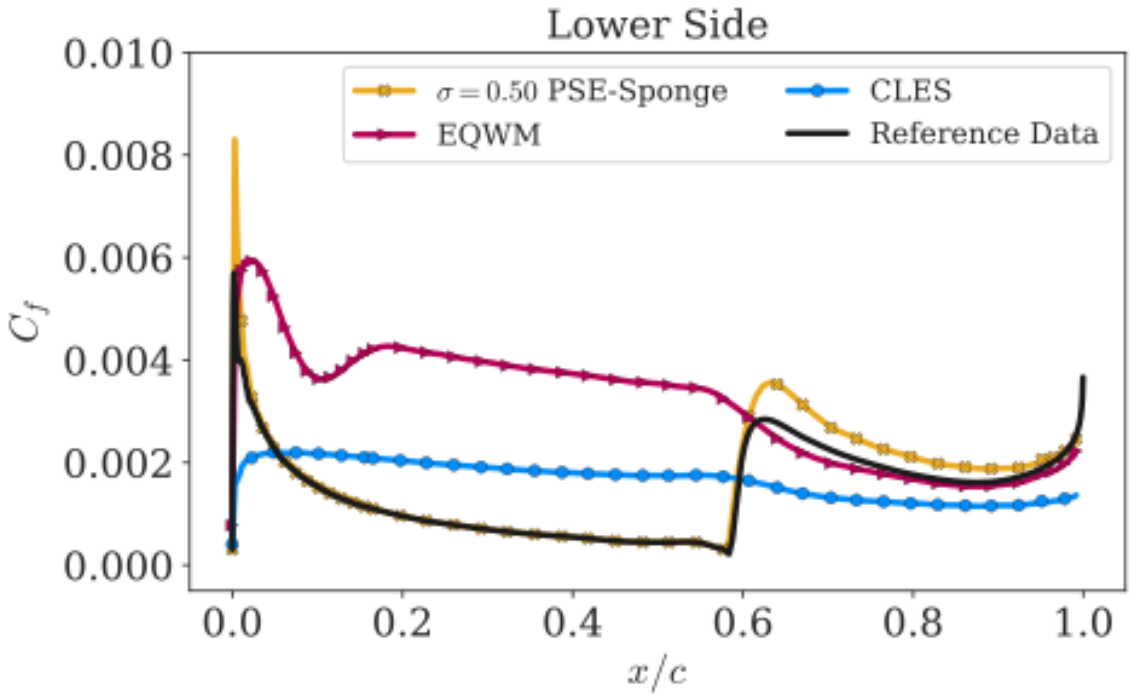


NLF PSE-Sponge Results

- CLES predicts fully laminar flow on upper and lower surfaces
- EQWM erroneously transitions near the leading edge
- PSE-Sponge is able to accurately predict the transition location and overall skin friction curve



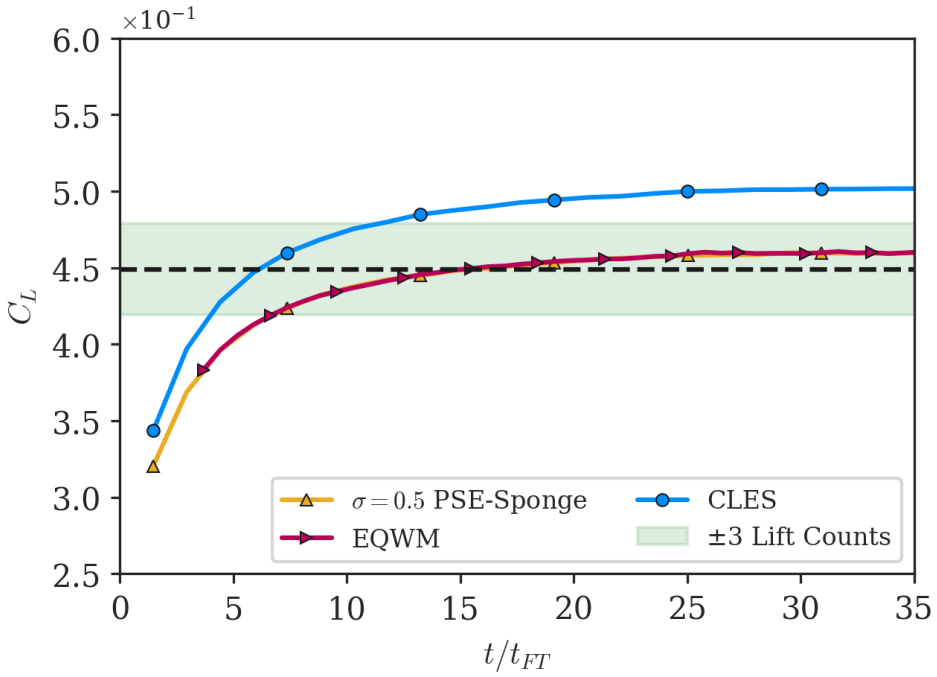




Griffin, K. P *et al.* (2024). Pressure-gradient-based RANS model for separation in transitional and turbulent flows. *Proceedings of the CTR Summer Program, Center for Turbulence Research, Stanford University*.

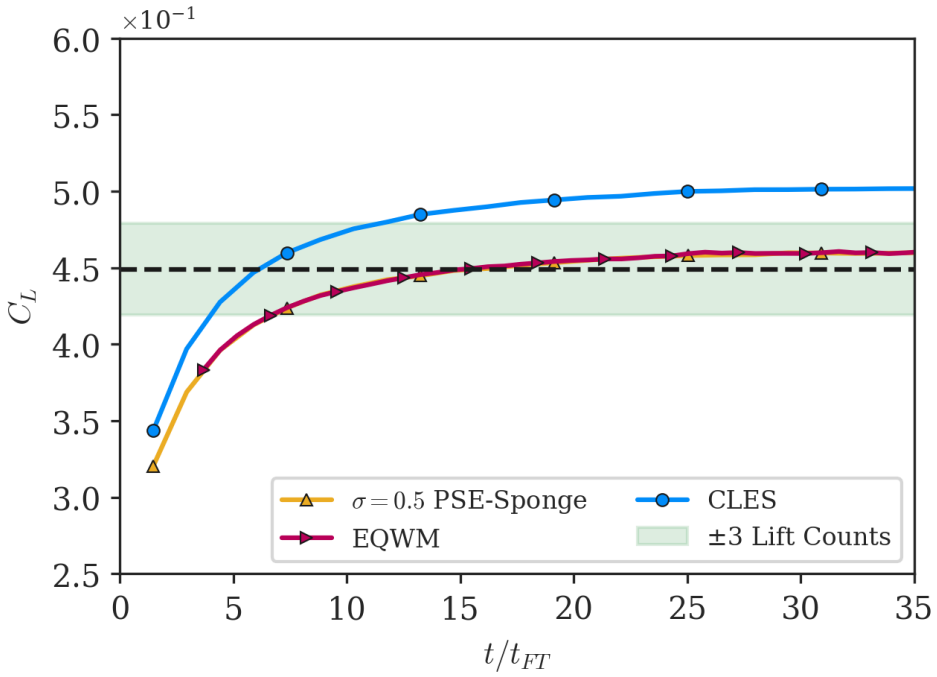
NLF PSE-Sponge Results

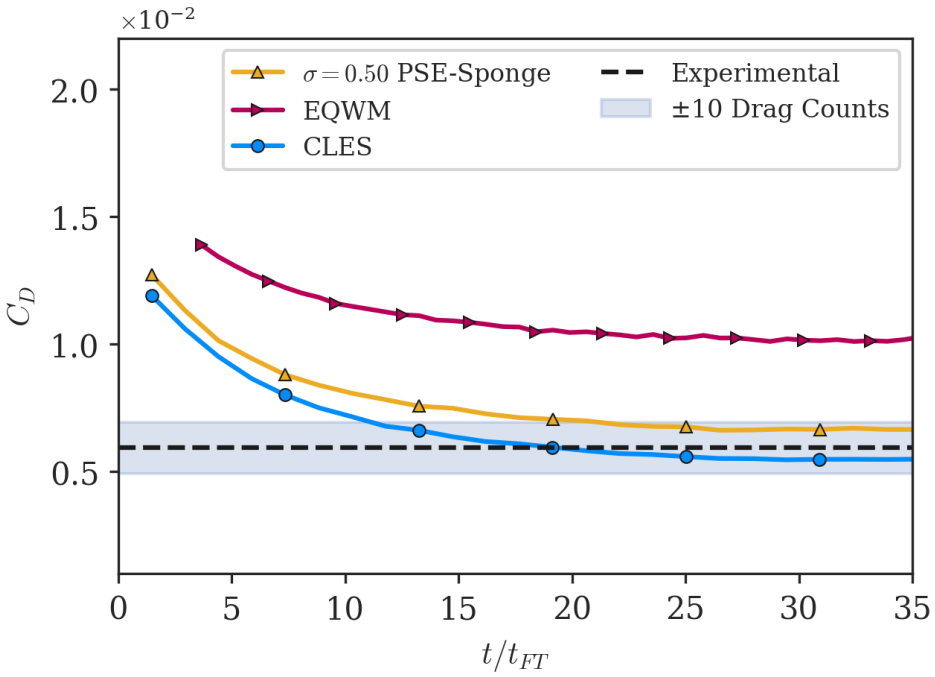
- Shaded box represents industry standard tolerances for CFD based predictions of mean quantities of interest
- CLES overpredicts the lift due to trailing edge effects



NLF PSE-Sponge Results

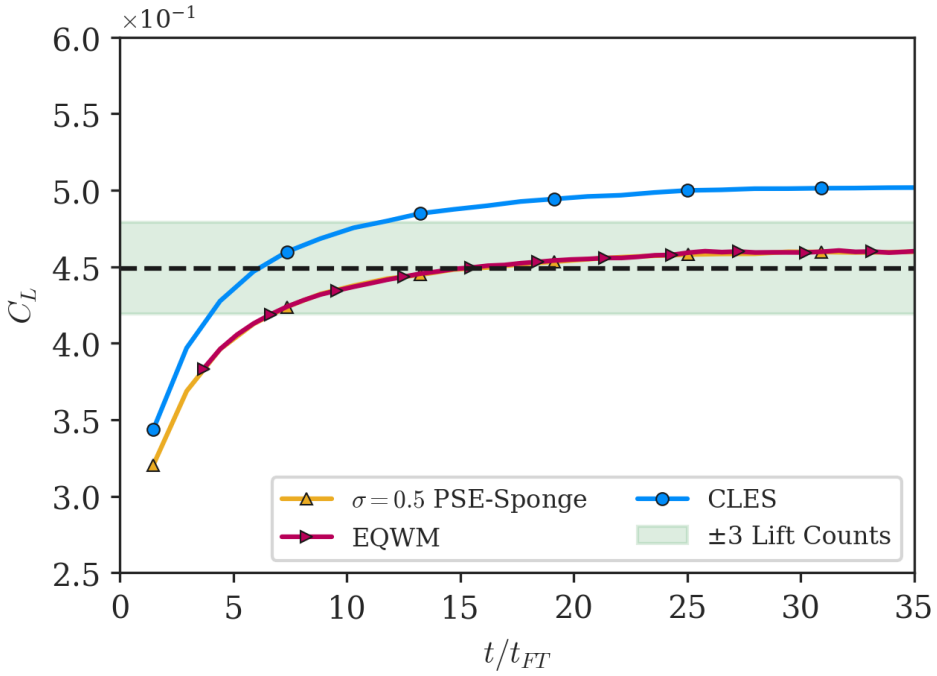
- Shaded box represents industry standard tolerances for CFD based predictions of mean quantities of interest
- CLES overpredicts the lift due to trailing edge effects
- EQWM over predicts drag due to fully turbulent flow

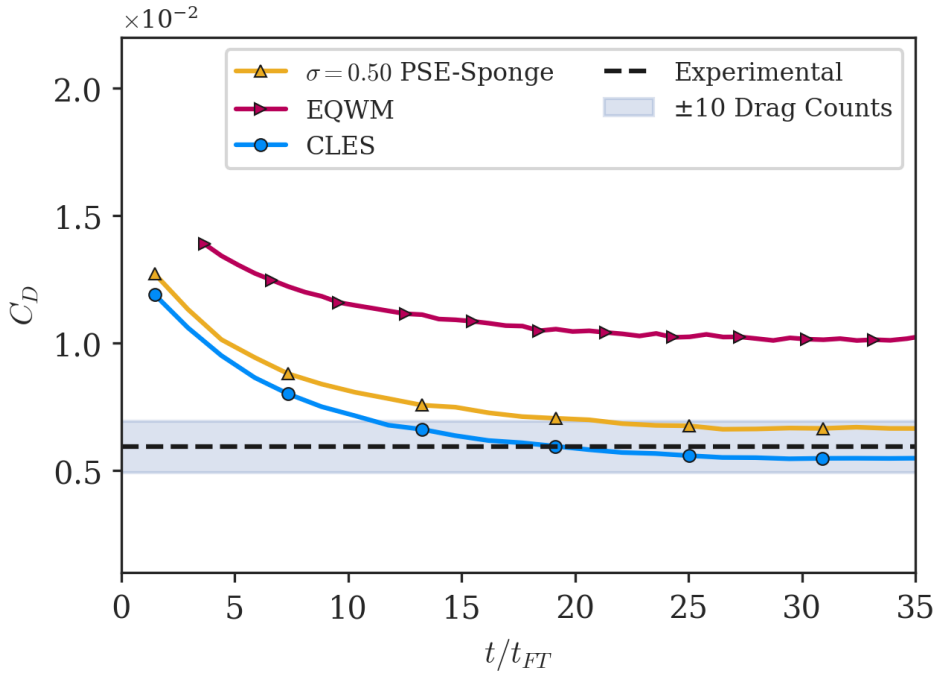




NLF PSE-Sponge Results

- Shaded box represents industry standard tolerances for CFD based predictions of mean quantities of interest
- CLES overpredicts the lift due to trailing edge effects
- EQWM over predicts drag due to fully turbulent flow
- PSE-Sponge is the only model that accurately predicts all quantities of interest!





Conclusions

- Development of the Falkner-Skan wall model
- Demonstrated NLPSE – WMLES inflow method for simulating transitional flows
- Developed PSE-Sponge method
- The new Hybrid NLPSE-WMLES approach was demonstrated to offer significant cost reduction while maintaining accuracy in the prediction of transition

The PSE--Sponge Method: An Approach for Simulating Natural Transition in Wall-Modeled Large-Eddy Simulations, JCP, under review

Thank you!

Questions?